SALAMANDRA **61**(4): 373–394
30 October 2025 | ISSN 0036–3375

SALAMANDRA
German Journal of Herpetology

A new species of Himalayan skink of the genus *Ablepharus* (Squamata: Scincidae)

Andrey M. Bragin[1,2], Ht. Decemson[2], Hmar Tlawmte Lalremsanga[2], Zeeshan A. Mirza[3] & Nikolay A. Poyarkov[4]

[1] Joint Russian-Vietnamese Tropical Research and Technological Center, Nghia Do, Cau Giay, Hanoi, Vietnam
[2] Developmental Biology and Herpetology Laboratory, Department of Zoology, Mizoram University, Aizawl, Mizoram, 796004, India
[3] Max Planck Institute for Biology, Max-Planck-Ring 1, 72076 Tübingen, Germany
[4] Department of Vertebrate Zoology, Biological Faculty, M. V. Lomonosov Moscow State University, Moscow 119234, Russia

Corresponding author: Andrey M. Bragin, ORCID 0000-0002-3621-9763, e-mail: bragin98@yandex.ru

Manuscript received: 11 April 2025
Accepted: 18 August 2025 by Andreas Schmitz

Abstract. Based on morphological and genetic evidence, we evaluated the taxonomic status of a deeply divergent highland population of Himalayan ablepharine skinks (genus *Ablepharus* Fitzinger in Lichtenstein, 1823) from Uttarakhand state in northern India. This lineage, here described as a new species, forms a well-supported clade of *Ablepharus* and differs from the morphologically similar species by a significant divergence in the 16S rRNA and cytochrome b mitochondrial DNA gene sequences. From the phylogenetic analysis of a 2,961 bp concatenated alignment of the ND2, cyt b, 16S, and 12S rRNA mitochondrial DNA genes and diagnostic morphological characters, we allocate the newly discovered population from Duggal Bittha village, Chopta region to the *A. tragbulensis-A. ladacensis* species complex (Clade 1 according to Bragin et al. 2024) and describe it as *Ablepharus flammeus* sp. n. Our discovery brings the number of *Ablepharus* species in India to seven and in the Himalayan region to eleven and emphasizes the incompleteness of knowledge on the herpetofaunal diversity of this highland region. In this study, we also compare known morphological data for ablepharine skinks from the Himalayan region and discuss the hidden cryptic diversity within this group of skinks.

Key words. Sauria, *Ablepharus*, biodiversity, India, morphology, phylogenetics, taxonomy.

Introduction

The Karakorum, Himalaya, and Tibet mountain systems are inhabited by at least eight species of the genus *Ablepharus*: *A. himalayanus* Günther, 1864, *A. sikimmensis* Blyth, 1854, *A. ladacensis* Günther, 1864, *A. tragbulensis* Alcock, 1898, *A. capitaneus* Ouboter, 1986 (according to Eremchenko et al. 1998, Bragin et al. 2024), *A. mahabharatus* Eremchenko, Shah & Panfilov, 1998, *A. nepalensis* Eremchenko & Helfenberger, 1998 (Uetz et al. 2024). Three of the aforementioned species have wide ranges spanning vast mountainous areas in the east (*A. himalayanus* and *A. ladacensis*) and west (*A. sikimmensis*) of the region. As is often the case with small members of the family Scincidae, ablepharine skinks have similar external morphologies (Chapple et al. 2023). However, from the outset of research on this group (see Bragin et al. 2024), it was evident that the focal taxa are comprised of cryptic species.

The taxonomic history of the species *A. ladacensis* and *A. himalayanus* is especially interesting. Günther (1864) described these morphologically distinct species as two independent species within the genus *Eumeces* Wiegmann, 1834. However, for unclear reasons, Ouboter (1986) considered them as part of a single species, *Scincella ladacensis*, and he relegated the latter to a subspecific status: *Scincella ladacensis ladacensis* and *S. ladacensis himalayana*. Ouboter (1986) further noted greater variability of morphological characters within the group. This later led to the reinstatement of the species status of *Asymblepharus himalayanus* (Eremchenko et al. 1998) and the description of two subspecies within *A. ladacensis* (Eremchenko 1992): *Asymblepharus ladacensis ladacensis* Eremchenko, 1992 from northwestern India and *Asymblepharus ladacensis stimsoni* Eremchenko, 1992 from Nepal. However, even in the latest, most complete morphological revision of the ablepharine skinks of Nepal (Eremchenko in Schleich & Kästle 2002), Eremchenko gives the following diag-

nosis for the *A. himalayanus* species: "Very variable–from small, slim lizards, for example a population of Simla (NW India, Himachal Pradesh State), some populations in Kashmir; to big wide-headed and long-tailed lizards from Gulmarg (Gulmarg, 2,704 m), Lidder (Lidar) Valley and Marri, all in Kashmir", with a wide range of not only metric but also meristic characters. Such a range of characters, wider than the morphological differences between recognized species, strongly hints at several hidden cryptic taxa within *Ablepharus* group. There have been no attempts to reconstruct the phylogeny of ablepharine skinks using molecular methods for a long time. However, the latest research by Bragin et al. (2024) proposes a molecular hypothesis of the relationships within ablepharine skinks based on a comprehensive sampling of taxa (encompassing 18 out of the 23 recognized ablepharine skink species), reconstructing four major clades inhabiting the Karakorum, Himalaya, and Tibet mountain systems, of which three belong to the genus *Ablepharus*, and the other one includes all known species of the genus *Protoblepharus*. Moreover, the analysis not only confirmed currently recognized species, but also reconstructed eight to ten additional, potentially new species-level lineages inside the *Ablepharus* group. These were found mainly within the broadly distributed and morphologically variable species *A. himalayanus* and *A. ladacensis*, which constitute cryptic species complexes. Thus, the obtained results of previous studies on this skink group show the underestimation of the taxonomic diversity of ablepharine skinks and help to outline a work plan for the future.

During our recent field surveys in Uttarakhand state of India, we encountered an unusual population of ablepharine skinks superficially similar to *A. himalayanus* in overall morphological habitus and body coloration. Closer morphological examination of scalation, patterns of coloration, and morphometric characteristics of this population demonstrated clear morphological differences from other representatives of *Ablepharus* inhabiting the Himalayas. In the present paper, we demonstrate that these differences are concordant with a significant divergence between mtDNA gene sequences among this population. Subsequent phylogenetic analyses of four mtDNA genes (ND2, cyt b, 16S, and 12S rRNA) confirmed the placement of the population from the highlands of Chopta region within *A. tragbulensis-A. ladacensis* species complex (Clade 1 according to Bragin et al. 2024), where this population forms a deeply divergent lineage. Therefore, in the present paper, we describe the *Ablepharus* population from the highlands of Uttarakhand, India as a new species and discuss the taxonomy of Himalayan ablepharine skinks.

Materials and methods

Collection

We used tissues from the herpetological collections of the Developmental Biology & Herpetology (DB&H) Laboratory of Mizoram University (MZMU, Aizawl, India) (summarized in Supplementary Table S1). For alcohol-preserved voucher specimens stored in museum collections, we removed a small sub-sample of muscle or liver, preserved it in 96% ethanol, and stored samples at -70 °C. We analyzed four tissue samples representing two newly discovered populations of *Ablepharus* inhabiting Uttarakhand state in northern India. In our analysis, we also included 281 GenBank sequences from ninety specimens of fifteen nominal *Ablepharus* species, six specimens of three nominal *Protoblepharus* species, and sixteen species of non-ablepharine outgroups used for rooting the phylogenetic tree (Supplementary Table S1). The geographic location of sampled *Ablepharus* populations is presented in Figure 1. The collected specimens were subsequently deposited in the following herpetological collections: holotype deposited in the herpetological collection of the Zoological Survey of India, Kolkata (ZSI), and paratypes deposited in the herpetological collection of the Developmental Biology & Herpetology (DB&H) Laboratory of Mizoram University (MZMU, Aizawl, India).

For all aspects of species concepts and delimitation, we follow the General Lineage Concept (sensu De Queiroz 2007), where a species represents a single evolutionarily independent lineage following a separate trajectory compared to its relatives. We specifically delimit evolutionary independence when lineages are reciprocally monophyletic, exhibit substantial genetic divergence, and are morphologically diagnosable.

Laboratory procedures

For molecular phylogenetic analyses, total genomic DNA was extracted from ethanol-preserved liver tissue using standard phenol-chloroform-proteinase K (final concentration 1 mg/ml) extraction procedures with consequent isopropanol precipitation (protocols followed by Russell & Sambrook 2001). For mtDNA, we amplified sequences covering the ND2 (mitochondrially encoded NADH dehydrogenase 2), cyt b (mitochondrially encoded cytochrome b), 16S rRNA, and 12S rRNA mtDNA genes to obtain a 2961 bp-length of continuous fragments of mtDNA. These fragments have also proven to be particularly useful in taxonomic studies of the ablepharine skinks and closely related taxa (Macey et al. 2006, Hedges 2014, Ankita et al. 2017, Che et al. 2020, Weng et al. 2021, Mirza et al. 2022, Bragin et al. 2024). In total, we amplified a 1,600 bp-long fragment of the ND2 gene, 406 bp-long fragment of the cyt b gene, 550 bp-long fragment of the 16S rRNA gene, and 405 bp-long fragment of the 12S rRNA gene. Primers used in PCRs and sequencing were taken from the literature and are summarized in Supplementary Table S2.

For primer pairs of the ND2 gene, we used the following PCR protocol: (1) initial denaturation step at 95 °C for 3 min; (2) 36 cycles of denaturation at 95 °C for 30 sec, annealing at 47 °C for 45 sec and extension at 72 °C for 1 min; (3) final extension at 72 °C for 10 min; and (4) cool-

ing step at 4 °C for storage. For primer pairs of the 16S rRNA gene: (1) initial denaturation step at 94 °C for 5 min; (2) 40 cycles of denaturation at 95 °C for 1 min, annealing at 47 °C for 1 min and extension at 72 °C for 1 min; (3) final extension at 72 °C for 10 min; and (4) cooling step at 4 °C for storage. For primer pairs of the 12S rRNA gene: (1) initial denaturation step at 95 °C for 3 min; (2) 36 cycles of denaturation at 95 °C for 30 sec, annealing at 47 °C for 45 sec and extension at 72 °C for 1 min; (3) final extension at 72 °C for 10 min; and (4) cooling step at 4 °C for storage. For cyt b sequences we used a modified PCR protocol with a touchdown: (1) initial denaturation step at 95 °C for 5 min; (2) 10 cycles of denaturation at 95 °C for 1 min, annealing for 1 min with temperature decreasing from 50 °C to 45 °C (with cool-down at 0.5 °C per each cycle) and extension at 72 °C for 1 min; (3) 30 cycles of denaturation at 95 °C for 1 min, annealing at 47 °C for 1 min and extension at 72 °C for 1 min; (4) final extension at 72 °C for 10 min; and (5) cooling step at 4 °C for storage. PCRs were run on a Bio-Rad T100TM Thermal Cycler; sequence data collection and visualization were performed on an ABI 3730xl automated sequencer (Applied Biosystems, Foster City, CA, USA). PCR purification and cycle sequencing were done commercially through Evrogen (Moscow, Russia). All unique sequences were deposited in GenBank (see Supplementary Table S1).

Genetic data analysis

In addition to newly obtained sequences, we also used 281 DNA sequences of Scincidae from GenBank in our final alignments; sequences of *Scincella* cf. *potanini*, *S. huanrenensis*, *S. modesta*, *S. vandenburghi*, *S. doriae*, *S. rupicola*, *S. melanosticta*, *S. reevesii*, *Sphenomorphus incognitus*, *S. indicus*, *Isopachys gyldenstolpei*, *Tropidophorus hangnam*, *Plestiodon chinensis*, *P. liui*, *P. elegans*, and *Ateuchosaurus chinensis* were selected as outgroup taxa to help root

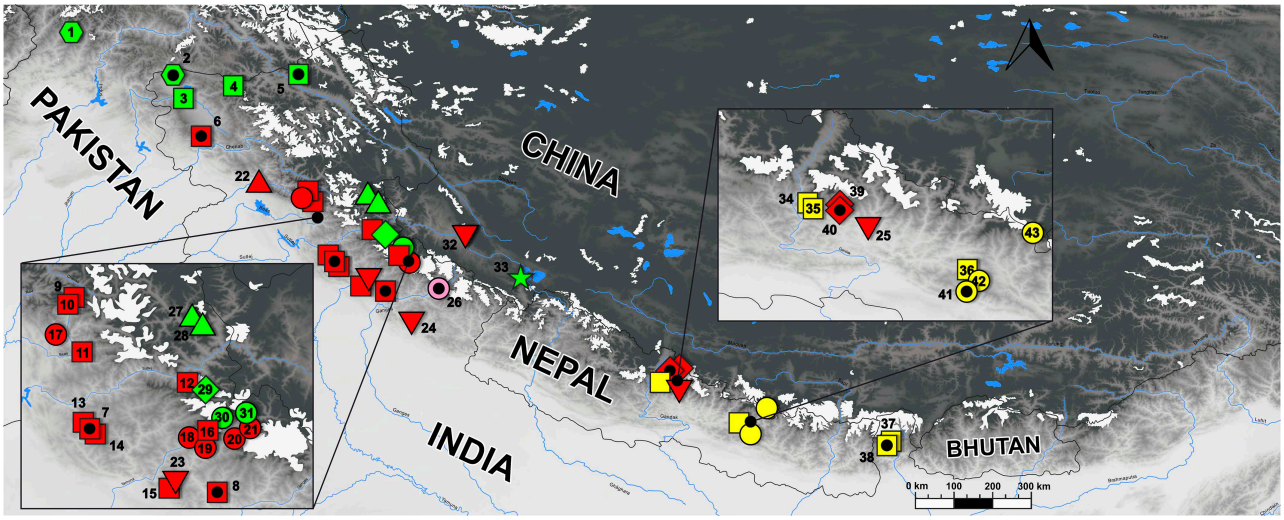

Figure 1. Map showing the distribution of the studied *Ablepharus* populations' locations. The shapes and colours of the figures correspond to those in the names of the samples in Figure 2. Conventions: a figure with a dot indicates the type localities of the corresponding species: pink circle – *Ablepharus flammeus* sp. n.; green hexagon – *A.* cf. *tragbulensis*, green square – *A. ladacensis* sp. 5; green triangle – *A. ladacensis* sp. 1; green diamond – *A. ladacensis* sp. 2; green circle – *Ablepharus* sp. 1; green inverted triangle – *A. ladacensis* sp. 3; green star – *A. ladacensis* sp. 4; red square – *A. himalayanus* sp. 1; red triangle – *A. himalayanus* sp. 4; red circle – *A. himalayanus* sp. 3; red diamond – *A. nepalensis*; yellow square – *Ablepharus sikimmensis*; yellow circle – *A. mahabharatus*; blue circle – *Protoblepharus* sp.; blue triangle – *P. apatani*; blue square – *P. medogensis*; blue diamond – *P. nyingchiensis*. Localities: 1 – Pakistan, Kumrat; 2 – India and Pakistan, Kashmir, Tragbul Pass, about 50 km NW from Srinagar; 3 – India, Jammu and Kashmir, Gulmarg; 4 – India, Jammu and Kashmir, Sonamarg; 5 – India, Ladakh; 6 – India, Kashmir; 7 – India, Himachal Pradesh, Shimla; 8 – India, Uttarakhand, Garhval; 9 – India, Himachal Pradesh, Manali; 10 – India, Himachal Pradesh, Naggar; 11 – India, Himachal Pradesh, Ghiagi; 12 – India, Himachal Pradesh, Batsari; 13 – India, Himachal Pradesh, Shimla; 14 – India, Himachal Pradesh, Chail; 15 – India, Uttarakhand, Rajaji National Park; 16 – India, Uttarakhand, Ful Chatn; 17 – India, Himachal Pradesh, Naragan; 18 – India, Uttarakhand, Ful Chatn; 19 – India, Uttarakhand, Nanketal; 20 – India, Uttarakhand, Seven Lakes; 21 – India, Uttarakhand, Dhorali; 22 – India, Himachal Pradesh, Chamba; 23 – India, Uttarakhand, Dehradun; 24 – India, Uttarakhand, Farsula; 25 – Nepal, Western region, Piple; 26 – India, Uttarakhand, Chopta; 27 – India, Himachal Pradesh, Dkhankhar; 28 – India, Himachal Pradesh, Dkhankhar; 29 – India, Himachal Pradesh, Chitkul; 30 – India, Uttarakhand, Seven Lakes; 31 – India, Uttarakhand, Dhorali; 32 – China, Tibet, Baidengpo; 33 – China, Tibet, Xizang; 34 – Nepal, Western region, Chomrung- Komrong Danda; 35 – Nepal, Western region, Damphus; 36 – Nepal, Central region, Gadawari; 37 – India, probably Sikkim; 38 – India, Sikkim; 39 – Nepal, Western region, Suikhet-Naudanda; 40 – Nepal, Western region, Pokhara, Phedi; 41 – Nepal, Central region, northern slopes of Mahabharat mountain range, along Bhainse-Pass Daman; 42 – Nepal, Central region, Gadawari; 43 – China, Tibet, Xigaze, Zhangmu (Khasa); 44 – India, probably Sikkim; 45 – India, Arunachal Pradesh, Talle; 46 – China, Tibet, Nyingchi; 47 – China, Tibet, Medog.

our tree. Details on taxonomy, localities, GenBank accession numbers, and associated references for all examined specimens are summarized in Supplementary Table S1.

Nucleotide sequences were initially aligned in MAFFT v6 (Katoh et al. 2002) with default parameters, subsequently checked by eye in BioEdit v7.2.5 (Hall 1999), and adjusted as needed. We reconstructed phylogenetic trees using a mtDNA concatenated dataset of ND2–cyt b–16S rRNA–12S rRNA fragments, used to assess species groups and estimate cryptic diversity within ablepharine skinks.

The optimum partitioning schemes for alignments were identified with PartitionFinder 2.1.1 (Lanfear et al. 2012) using the greedy search algorithm under an AIC criterion. Phylogenies were hypothesized via maximum likelihood (ML) and Bayesian Inference (BI). We used IQ-TREE (Nguyen et al. 2015) to reconstruct ML phylogenies. Confidence in tree topology for ML analysis was assessed by 1,000 bootstrap replications for ML analysis (ML BS). Bayesian inference (BI) was performed in MrBayes v3.1.2 (Ronquist & Huelsenbeck 2003). Metropolis-coupled Markov chain Monte Carlo (MCMCMC) analyses were performed and run with one cold chain and three heated chains for one million generations and sampled every 1000 generations. Five independent MCMCMC run iterations were performed and 1,000 trees were discarded as burn-in. Nodal support was assessed by calculating posterior probabilities (BI PP). The best-fitting model for both BI and ML analyses of the ND2, 12S rRNA, and 16S rRNA gene suggested by the AIC was the GTR+I+G model. For cyt b gene, following the AIC, the GTR+I+G model was used for the first codon partition, the GTR+G for the second codon partition, and the SYM+I+G for the third codon partition.

We *a priori* regarded tree nodes with BI PP values over 0.95 and ML BS values 75% or greater as sufficiently resolved, while BI PP values between 0.95 and 0.90 and ML BS values between 75% and 50% were regarded as tendencies. Lower values were regarded as indicating unresolved nodes (Huelsenbeck & Hillis 1993).

Species delimitation

Based on the Assemble Species by Automatic Partitioning (ASAP; Puillandre et al. 2021) species delimitation method, we examined putative species boundaries beyond those currently recognized by taxonomists. Barcode gaps, presumably occurring between intra- and interspecific distances, were separately used to partition the 16S rRNA and cyt b datasets into species hypotheses (initial partition). Resulting inferences were then recursively applied to yield finer partitions (recursive partitions) until no further partitioning was possible. ASAP analysis was run on the 16S rRNA and cyt b datasets through a web-based interface (https://bioinfo.mnhn.fr/abi/public/asap/#) using default parameters (Simple Distance (p-distances)). In addition, both inter- and intraspecific uncorrected genetic p-distances were calculated using MEGA X for the 16S rRNA and cyt b datasets (Kumar et al. 2018).

Morphological data analysis

Measurements were acquired using digital calipers X-PERT Xp150 to the nearest 0.1 mm. Measurements of type series were modified from Ouboter (1986), Das et al. (1998) and Grismer et al. (2019), including snout–vent length (SVL), from the tip of the rostral scale to the vent; tail length (TaL), from the vent to the tip of the tail; tail width (TaW), measured at the base of tail; axilla-groin length(AGD), measured from the posterior margin of the forelimb to the anterior margin of the hind limb; head length (HL1), from the tip of the snout to the angle of jaws from the lateral view; head length (HL2), from the tip of the snout to the posterior parietal from the dorsal view; interorbital distance (IOD), the distance between anterior edges of the orbits from the dorsal view; snout–ear length (SEL), from the tip of the snout to the anterior margin of the ear opening; head width (HW), the widest point of the head posterior to the eyes; head height (HH), the highest part of the head posterior to the eyes; body width (MBW), the widest point of the body closer to the hind limbs; internarial distance (IN), the distance between inner edges of nares from the dorsal view; eyeball diameter (ED), the anterior to the posterior margins of the eyeball; tympanum diameter (TD), measured as the longest length across the ear opening; rostral width (RW), the greatest distance between the lateral edges of the rostral scale; rostral height (RH), the greatest distance between the anterior and posterior edges of the rostral scale; snout length (SNL), from the tip of the snout to the anterior border of the orbit; eye–tympanum length (EED), from the posterior margin of the orbit to the anterior margin of the ear opening; eye–nostril length (END), from the margin anterior of the orbit to the posterior margin of the nares; snout–forelimb length (SNL), from the tip of the snout to the anterior margin of the forelimb insertion on the body; forelimb length (FLL), from the insertion point of the forelimb on the body to the tip of the fourth finger on an outstretched limb; hindlimb length (HLL), from the insertion point of the hindlimb on the body to the tip of the fourth toe on an outstretched limb; tibia length (TBL), measured along flexed tibia from the knee bend to the base of the pes; and length of the fourth toe of the hind limb (T4L). We also provide the following ratios: HL2/SVL; HW/SVL; HD/HL2; SNL/HW; ED/SNL; ED/HL2; SVL/BW; EED/END; SVL/HW; SVL/HL2; SVL/FLL; SVL/HLL so as to compare our data with data in Ouboter (1986) and Das et al. (1998). The metric characteristics of juvenile specimens were not taken into account.

Scale counts were made on the right or each side of the body under a Nikon SMZ460 stereo zoom microscope. Scale counts taken were the number of supraoculars contacted by the frontoparietal (F-SO); the degree of contact of prefrontals with each other, and with the frontal (PF); the number of nuchal scales on each side of the head (Nu) counted the number of enlarged scales (one and a half times larger than the dorsal scales), located immediately behind the parietals and interparietal and running

along the dorsal surface of the neck; number of primary, secondary, and tertiary temporals (PT, ST, and TT, respectively); the character of overlapping of the temporal and parietal scales; number of supraciliary scales (SC), supraoculars (SO), loreals (AL, PL), preoculars (PR), presuboculars (PRS), postoculars (PO), postsuboculars (PSO), supralabials (SL) and infralabials (IF) on each side of the head; number of projecting ear lobules (PEL) counted as a number of large granules noticeably protruding above the edge of the ear opening; character of the scalation of the lower eyelid and transparent window; number of midbody scale rows (MBSR) counted as the number of longitudinal scale rows encircling the body at a point midway between the limb insertions; paravertebral scale rows (PVSR) counted as the number of scales in a line from parietals to a point on the dorsum opposite the vent; dorsal scales rows (DBR), counted between the dorsolateral dark stripes; ventral scale rows (VSR) counted as a row of scales between the postmental and the precloacal scales; number of enlarged precloacal scales (PrC); fourth toe and finger subdigital lamellas (TL4 and FL4, respectively); the degree of contact between adpressed forelimb and hindlimb (F-H) and adpressed hind limbs and elbows (F-E); size and arrangement of rows of scales on the inner thighs (FemS); size (enlarged or not relative to adjacent scales) of subcaudal scales.

The hemipenes of the holotype are described according to Vergilov et al. (2017) and Vergilov & Zlatkov (2024). Color pattern characters included the presence or absence of dark vertebral, dorsolateral, and lateral stripes (continuous or breaking into separate spots forming a dotted line); the presence or absence of white lateral stripes bordering the lower edge of the dark lateral stripe (or their breaking up into separate spots forming a dotted line); general background coloration of the dorsum and venter, and venter of males (or/and females) during the mating season; the presence or absence of a white stripe under the eye; coloration of the crown of the head; presence or absence of subcaudal banding; presence or absence of spots on the dorsal and along lateral sides of the body.

Nomenclatural acts

The electronic edition of this article conforms to the requirements of the amended International Code of Zoological Nomenclature, and hence the new names contained herein are available under that Code from the electronic edition of this article. This published work and the nomenclatural acts it contains have been registered in ZooBank, the online registration system for the ICZN. The LSID (Life Science Identifier) for this publication is: urn:lsid:zoobank.org:pub:145737E5-5D28-4AFF-A923-A3565253B3AD. The electronic edition of this work was published in a journal with an ISSN and has been archived and is available from the following digital repositories: www.zenodo.org and www.salamandra-journal.com.

Results

Sequence characteristics

Our aligned matrix of all mtDNA data comprised 2.961 bp (assembled from 1.600 bp fragment from ND2, 406 bp fragment from cyt b, 550 bp fragment from 16S rRNA, and 405 bp fragment from 12S rRNA). It included 92 samples, representing 17 species of *Ablepharus* (75% of the currently recognized species, including 86% of the species that inhabit the Himalayas and two newly described species), three species (of three currently recognized species) of the phylogenetically closely related genus *Protoblepharus*, and 16 samples from outgroup taxa (see Table S1). Information on fragment lengths and variability is summarized in Table S3. PartitionFinder 2.1.1 proposed the partition schemes and substitution models, summarized in Supplementary Table S3. We deposited the newly obtained sequences in GenBank under the accession numbers PV097228–PV097229 (cyt b), PV097230–PV097231 (ND2), PV105692–PV105692 (16S), and PV105694–PV105695 (12S) (see Table S1).

Phylogenetic relationships

BI and ML phylogenetic analyses resulted in almost identical topologies (Fig. 2). The topology of the matrilineal genealogy was largely consistent with the phylogeny of ablepharine skinks presented by Bragin et al. (2024) and recovered five main clades grouped into two major reciprocally monophyletic groups, corresponding to the genera *Ablepharus* and *Protoblepharus* (Fig. 2). Monophyly of the genus *Ablepharus* was poorly supported in BI analysis, but had significant support in ML analysis (0.6/97, hereafter node values given for BI PP/ML UFBS, respectively; Fig. 2) as well as monophyly of the genus *Protoblepharus* (-/99); *Ablepharus* group included four strongly supported clades, three of which included species inhabiting the mountain systems of Tibet, the Himalayas, the Hindu Kush and the Karakoram

(1) Clade 1 (0.9/82) included two subclades mainly corresponding to two nominal species of *Ablepharus* inhabiting the Western Himalaya region and the Karakoram Mountain system: *A. tragbulensis* and *A. ladacensis*. The first subclade (0.91/81) included three relatively deeply divergent mitochondrial lineages with all nodes strongly supported (1/100): two specimens of *A. tragbulensis* from Karakoram, Pakistan; four specimens of *Ablepharus* sp. 1 from the northwestern part of Uttarakhand, India; and, including two specimens of *Ablepharus* sp. n. from newly discovered population from Chopta in the central part of Uttarakhand, India. The second subclade (1/99) included five mitochondrial lineages, corresponding to *A. ladacensis* species complex.

(2) Clade 2 (0.73/86) also included two subclades mainly corresponding to two nominal species of *Ablepharus* inhabiting the Western and Central Himalaya region: *A. nepalensis* and *A. himalayanus*. The first subclade (1/100) included specimens of *A. nepalensis* from a type locality in

Central Nepal, and the second subclade (0.51/95) included five mostly strongly supported mitochondrial lineages, corresponding to *A. himalayanus* species complex.

(3) Clade 3 (0.99/98) joined two species of *Ablepharus* from Central and Eastern Himalayas regions: *A. mahabharatus* and *A. sikimmensis*. The population of *Ablepharus*

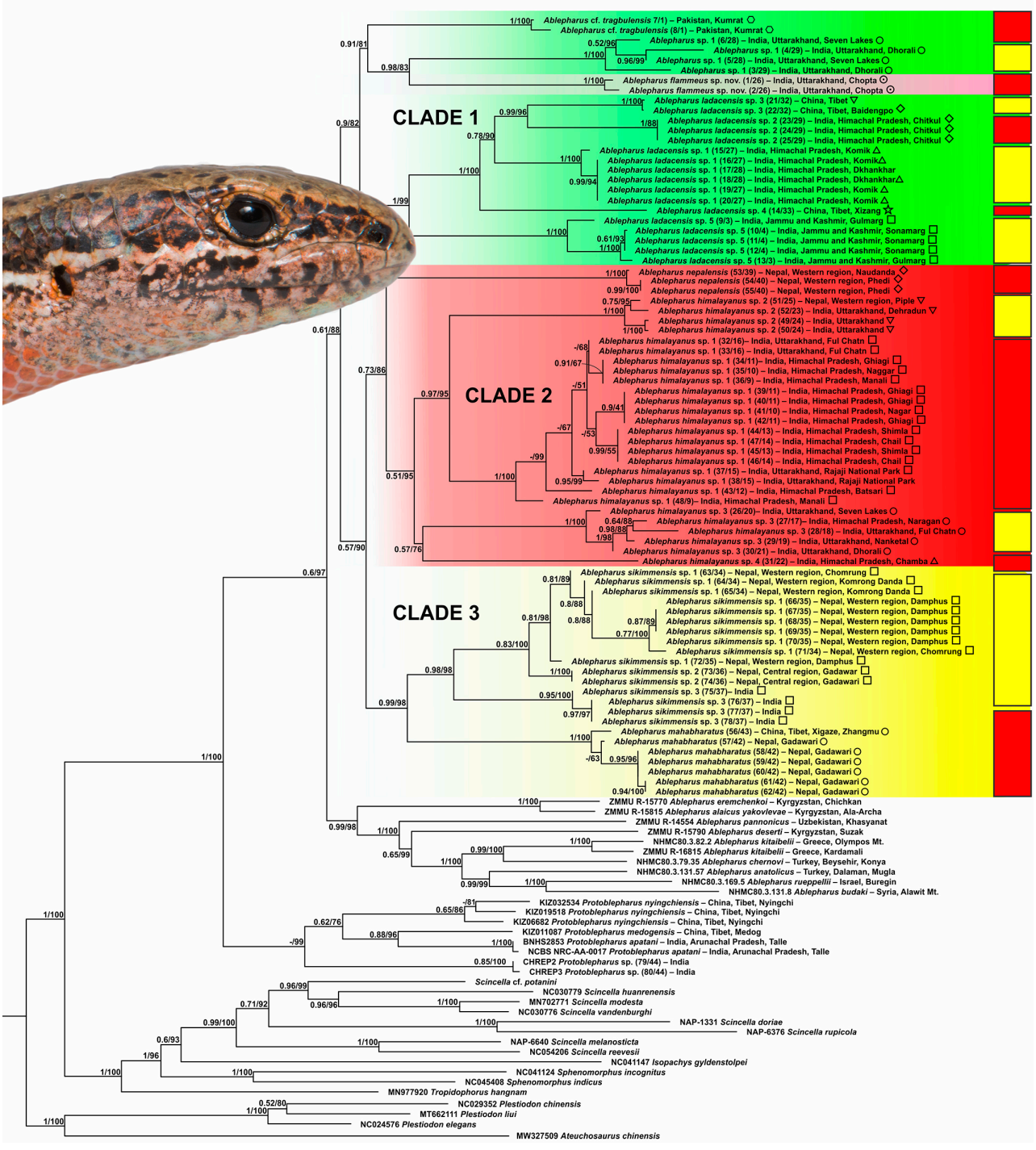

Figure 2. Molecular phylogeny plotted on the Maximum-Likelihood consensus tree based on mtDNA sequences (ND2, cyt b, 16S rRNA and 12S rRNA genes) of Himalayan snake-eyed skinks and congeners. Support values on branches are posterior probabilities (PP) resulting from a separate partitioned Bayesian analysis followed by ML bootstraps. Colour bars on the right of each clade correspond to the results of species delimitation analyses based on ASAP. The numbers in brackets correspond to the sample data/locality number in Table 1 and on the map in Figure 1. The figures in sample names and colours of the clade's selection correspond to those on the map in Figure 1. Inset photograph of *Ablepharus flammeus* (Uttarakhand, Chopta) by Andrey M. Bragin.

sp. n. under study from Chopta, Uttarakhand, India, belongs to clade 1 (Fig. 2), where it is reconstructed as a member of a subclade also including *A. tragbulensis* from Pakistan and *A.* sp. 1 from northwestern Uttarakhand, India. However, the monophyly of this subclade appears to be insufficiently resolved and had strong support in BI-analysis but was poorly supported in ML-analysis (0.91/81). Three included lineages all had strong node support (1/100).

Genetic distances

The uncorrected p-distances for the 16S rRNA and cyt b gene fragments among examined members of the genus *Ablepharus* are presented in Table S4. For the 16S gene, interspecific distances among the members of the genus *Ablepharus* varied from p = 1.8% (between *A. alaicus* and *A. eremchenkoi*) to p = 13.2% (between *A. ladacensis* sp. 4 and *A. anatolicus*); for the cyt b gene, interspecific distances varied from p = 7.5% (between *A. alaicus* and *A. eremchenkoi*) to p = 24.7% (between *A. deserti* and *A himalayanus* sp. 2). The newly discovered *Ablepharus* sp. n. lineage from Chopta is highly divergent from other congeners with the minimal genetic distance of p = 5.5% (with *A. sikimmensis* sp. 2) and the maximal distance of p = 11.6% (with *A. budaki*) of sequence divergence in 16S rRNA mtDNA gene; and with the minimal genetic distance of p = 14.6% (with *A. ladacensis* sp. 3) and the maximal distance of p = 22.0% (with *A. budaki*) of sequence divergence in cyt b mtDNA gene.

To assess the number of putative species-level lineages within the ablepharine skinks, we implemented the distance-based ASAP species delimitation analysis for the 16S rRNA and cyt b gene fragments. The result of ASAP analysis did not differ for the two mtDNA genes, resolved all the currently recognized species of the ablepharine skinks of the Himalayas region, and agreed well with recent ASAP results for this group (Bragin et al. 2024). ASAP analysis clearly recovered recently identified species-level lineage from the Chopta in Uttarakhand, India.

Systematics

Our molecular results are further corroborated by the morphological analysis, which recovered a number of important diagnostic characters that allow distinguishing the populations of *Ablepharus* sp. n. from the Chopta, Uttarakhand, India and all other congeners (summarized below). These results support our hypothesis that this recently discovered lineage of *Ablepharus* sp. n. from Uttarakhand, India represents a previously unknown species, which we formally describe below.

***Ablepharus flammeus* sp. n.**

Figs 5–7

ZooBank LSID: urn:lsid:zoobank.org:act:A6EB3BF4-EFF6-4E93-B2C8-3AABCC188A09

Holotype: ZSI-R-29457 (field no. BAM-171) (Figs 3, 5, 6, 7), adult male, collected by Andrey M. Bragin on 29 October 2022 from Duggal Bittha, Chopta, Uttarakhand, India (30.48° N, 79.17° E) at an elevation of 2,520 m a.s.l.

Figure 3. Holotype of *Ablepharus flammeus* sp. n. (ZSI-R-29457, male) in life. Photograph by Andrey M. Bragin.

Paratypes: Six males, one female, and two juveniles. Males: MZMU3657, MZMU3652, MZMU3658, MZMU3659, and MZMU3653 (field no. BAM-170, BAM-172, BAM-173, BAM-174, and BAM-175, respectively) collected on 29 October 2022 from Duggal Bittha, Chopta, Uttarakhand, India (30.48° N, 79.17° E) at an elevation of 2,520 m a.s.l.; MZMU3660 (field no. BAM-176) collected on 29 October 2022 from the vicinity of Tungnath Temple, Chopta, Uttarakhand, India (30.48° N, 79.20° E) at an elevation of 3,305 m a.s.l. Female: MZMU3656 (field no. BAM-169) collected on 29 October 2022 from Duggal Bittha, Chopta, Uttarakhand, India (30.48° N, 79.17° E) at an elevation of 2,520 m a.s.l. Juveniles: MZMU3654 and MZMU3655 (field no. BAM-167 and BAM-168, respectively) collected on 29 October 2022 from Duggal Bittha, Chopta, Uttarakhand, India (30.48° N, 79.17° E) at an elevation of 2,520 m a.s.l. Andrey M. Bragin collected all the above specimens.

Figure 4. The type locality of *Ablepharus flammeus* sp. n. in the vicinity of Chopta, Uttarakhand, India: (A) Gentle slopes covered with multilayer high-stem polydominant deciduous forests formed by *Quercus semecarpifolia, Q. floribunda, Acer acuminatum, Aesculus indica, Q. leucotrichophora* and *Alnus nepalensis* at an altitude of 2520 m a.s.l.; (B) steep slopes covered with patches of low mixed forest formed by *Abies pindrow*, *Quercus semecarpifolia, Q. floribunda, Rhododendron arboreum,* etc. grading into subalpine and alpine meadows. Photographs by Andrey M. Bragin.

Etymology: The specific epithet of the new species "*flammeus*" is an adjective in nominative singular, in masculine gender, formed from the Latin words "*flamma*", meaning "fire". The name of the new species reflects the fiery coloration of the neck, belly, inner thighs, forearms, and the ventral part of the tail in males and juveniles, as well as the intense yellow coloration of these body parts in females. Notably, these small ectothermic lizards thrive at high altitudes exceeding 3,000 meters above sea level, with some individuals observed basking near the edges of snowfields. The name also symbolizes the ardent disposition of these lizards and their resilient struggle for survival. Furthermore, the species' habitat lies near the Tungnath Temple – the highest mountain temple dedicated to the god Shiva – which also serves as the type locality for the species. Fire, as one of Shiva's symbols, represents both destruction and the fight for life, reinforcing the essence of the species' name. We propose "Fire-bellied Ground Skink" as the English common name, "Ognennobryukhii gologlaz" ("Огненнобрюхий гологлаз") as the Russian common name, and "Laiteldulsen" as the Mizo common name for this species.

Diagnosis: *Ablepharus flammeus* is a medium-sized, robust ablepharine skink with (1) snout–vent length (SVL) 41.6–50.6 mm; (2) head length (HL2) 7.7–9.1 mm; (3) tail length (TaL) 52.6–68.3 mm; (4) head, body, and caudal scales smooth; (5) supranasals absent; (6) nasal semi-divided; (7) the lower eyelid is movable, covered with small arranged granules and with large transparent window; (8) tympanum rounded, deeply sunk, with one (70%), two (20%) or three (10%) projecting lobules on the anterior border; (9) prefrontals two, separated by frontonasal and frontal or, rarely, prefrontals touch at one point; (10) frontal elongated, in contact with 1st and 2nd supraoculars laterally, rarely in contact with 3rd supraoculars; (11) frontoparietals two; (12) interparietal large, diamond-shaped, slightly elongated posteriorly, in contact with frontoparietals anteriorly and parietals posteriorly; (13) parietals in contact posterior to interparietal, not divided; (14) supraoculars four; (15) supralabials seven; (16) infralabials six; (17) chin shields in four pairs; (18) eight nuchals in four pairs behind parietals; (19) followed by four transverse dorsal rows between dorsolateral dark stripes, all similar in size; (20) 50–52 paravertebral scales rows; (21) 52–56 ventral longitudinal rows (including gulars); (22) 26–28 midbody scale rows; (23) two enlarged precloacals; (24) the central subcaudal row enlarged; (25) 12 subdigital lamellae beneath fourth finger; (26) 16 subdigital lamellae beneath fourth toe; (27) femoral scales large and oriented longitudinally; (28) dorsum brown, with absent or rarely dotted two dark vertebral stripes; (29) two dark dorsolateral stripes; (30) venter, lower flanks, ventral region of the neck, tail, and limbs of males and juveniles from orange to red, and yellow in females.

Description of holotype: An adult male in a good state of preservation with a 25 mm long mid-ventral incision. The hemipenes of the specimen are fully everted to determine the sex of the specimen and for description. The specimen

is preserved in a linear manner; limbs are curved slightly inward and backward.

Snout–vent length (SVL) 41.6 mm; tail length (TaL) 62.4 mm; total length 104 mm; snout acute in dorsal and lateral aspects (EED/END ratio 1.57), slightly projecting beyond lower jaws; nostril with lateral orientation, slightly oval, posterior edge oriented diagonally upward, situated much closer to the snout tip than to the eye (END/SNL ratio 0.71); head robust, longer than wide (HL2/HW ratio 1.14). Body slender (SVL/MBW ratio 5.9); head not distinct from the neck, but cervical interception weakly expressed in front of the attachment point of the forelimbs. Forelimbs and hindlimbs are relatively short and stout (SVL/FLL ratio 3.67; SVL/HLL ratio 2.65), normally developed, each with five fingers, the tips of digits of forelimb and hindlimb not meeting when the limbs are adpressed against each other along the body axis, adpressed hind limbs not reaching elbows when the hind limbs are adpressed (Fig. 5); forearm very short (ForL/SVL ratio 0.08); tibia longer than forearm (TibL/SVL ratio 0.12); digits moderately long, slender and ending with distinctly visible, sharp, thin, slightly curved, and pointed claws (Figure 5). Subdigital lamellae smooth on manus and pes, entire; number of subdigital lamellae without taking into account claw sheath: right manus 6-10-12-12-8; right pes 4-9-12-16-10. Relative lengths of digits (measurements in parentheses in mm): left manus IV > III >V > II > I; left pes IV (3.4 mm) > III (3.1 mm) > V (2.8 mm) > II (2.6 mm) > I (1.2 mm). Scales on dorsal and ventral surfaces of the limbs are smooth and imbricate, femoral scales are large and oriented longitudinally. Scales on the palmar and plantar regions much smaller than the associated digit lamellae and the scales on ventral surfaces of limbs; rounded or slightly elongated, smooth, and subimbricate. Other measurements and ratios of the holotype and paratypes are given in Tables 1, 2.

Rostral wider (1.9 mm) than high (1.1 mm), in contact with first supralabials, nasals and frontonasal (Figs 5, 6). A pair of nasals not in contact with each other. Nasal posteriorly in contact with slightly smaller anterior loreal; laterally widely in contact with first supralabials. A large single frontonasal in broad contact with the rostral anteriorly and the frontal posteriorly; widely in contact with nasal, the anterior loreal, and prefrontal laterally. A pair of prefrontals separated by the frontal. Prefrontal anteriorly in contact with frontonasal, posteriorly in contact with frontal, first supraocular, and first supraciliary scale, laterally in contact with anterior and posterior loreals. Frontal large, nearly twice longer than wide, irregularly pentagonal with slightly rounded tapering posterior margin, contacting frontonasal and prefrontals anteriorly, in wide contact with first and second supraoculars laterally, in wide contact with frontoparietals posteriorly. Frontoparietals widely in contact with parietals and interparietal scale posteriorly, contacting frontal and second, third and fourth supraoculars anterolaterally. Interparietal rhomboid, posteriorly in contact with parietals; parietal eye indistinct. Parietals anteriorly in contact with frontoparietals, interparietal and fourth supraoculars; laterally touching upper secondary temporal, upper and lower pretemporals; in contact with two pairs of nuchals posteriorly. Parietal overlapping upper secondary temporal.

Four supraoculars, the second being the largest, decreasing in size in both directions (Figs 5, 6). Scales on the lateral aspect of the head bear pits, throughout their surface and dispersedly placed. The density of the pits on the scales is rare on dorsal head scales and barely noticeable towards the posterior borders of parietals (Figs 5, 6). Nostril with lateral orientation slightly oval, posterior edge oriented diagonally upward, located closer to the posterior edge of nasal. Nasal semi-divided, the groove runs from the central posterior edge of the nostril to the posterior edge of the nasal. Postnasals absent. Anterior and posterior loreals roughly quadrangular, posterior loreal wider than anterior loreal; anterior loreal anteriorly in contact with nasal and frontonasal, posteriorly in contact with posterior loreal and prefrontal, laterally in contact with first and second supralabials; posterior loreal anteriorly in contact with anterior loreal and prefrontal, posteriorly in contact with first supraciliary scale and two preoculars, laterally in contact with second and third supralabials. Three preoculars, the upper one smaller than the lower one; one presubocular, slightly larger than the middle preocular (Figs 5, 6). The upper eyelid bordered by five supraciliary scales and seven ciliary scales; and the lower eyelid with nine ciliary scales; the scales covering the lower eyelid are small, round, granule-like, spaced apart from each other; the lower eyelid bears oval, horizontally oriented, large transparent window. The upper edge of the transparent window is practically in contact with the lower edge of the ciliaries, almost half of the horizontal diameter of the orbit long (0.35 mm high, 0.59 mm wide, ED/transparent window wide ratio 2.29). Seven supralabials, gradually increasing in size, with the fifth and sixth supralabials being the largest; fifth supralabials forming the lower border of the eyelid. Two small equal-sized postoculars anteriorly in contact with the last supraciliary scale and in touch at one point with the last supraocular, posteriorly in contact with upper and lower pretemporals, laterally in contact with upper postsuboculars. Three postsuboculars, where the middle one is the largest, posteriorly in contact with lower pretemporal and primary temporal, laterally in contact with lower postoculars and fifth and sixth supralabials. One large rhomboid primary temporal anteriorly in contact with lower pretemporal, two postsuboculars and sixth supralabial, posteriorly in contact with upper and lower secondary temporals and seventh supralabial. Two secondary temporals, the upper one larger than the lower one. Parietal and lower secondary temporal overlap upper secondary temporal. Secondary temporals anteriorly in contact with parietal, lower pretemporal, primary temporal and seventh supralabial, posteriorly in contact with nuchal, upper and lower tertiary temporals and upper postsupralabial. Two tertiary temporals, approximately the same size. The lower one overlapping the upper one. Two, equal-sized, posteriorly elongated postsupralabials behind the seventh supralabial. One row of large scales between postsupralabials and the anterior edge of the ear opening. The ear opening is large, slightly oblate in front

Table 1. Morphological measurements (in mm) and proportions for the type series *Ablepharus flammeus* sp. n. Abbreviations are listed in the Materials and methods. n.a. – data unobtainable or not applicable; * – regenerated tail.

	ZSI-R-29457	MZMU3656	MZMU3657	MZMU3652	MZMU3658	MZMU3659	MZMU3653	MZMU3660	MZMU3654	MZMU3655
	Holotype	Paratype	Paratype	Paratype	Paratype	Paratype	Paratype	Paratype	Paratype	Paratype
	♂	♀	♂	♂	♂	♂	♂	♂	Juv	Juv
SVL	41.6	50.6	44.6	44.8	45.5	43.4	47.3	46.4	29.2	28.4
TaL	62.4	n.a.	68.3	53.3	52.6	39.7*	59.1	36.8*	43.9	39.9
TaW	4.0	4.2	3.7	5.3	4.6	4.3	4.2	4.4	2.6	2.9
AGD	24.4	31.3	27.3	29.4	28.9	26.3	27.1	26.0	16.9	17.3
HL1	8.2	8.0	7.7	5.1	7.3	7.7	5.5	7.4	5.5	5.3
HL2	7.7	8.4	8.5	9.1	8.5	8.3	8.6	8.5	6.7	6.0
IOD	3.2	3.5	3.5	4.0	3.8	3.2	4.3	3.4	2.6	2.5
SEL	8.5	9.0	9.0	9.3	9.1	8.8	9.4	9.2	6.8	6.2
HW	6.7	6.2	6.6	6.0	6.6	6.2	7.1	6.8	4.8	4.7
HH	3.9	4.3	4.7	4.5	5.3	5.3	5.7	5.0	3.3	3.3
MBW	7.0	8.3	8.1	6.3	7.3	7.2	7.3	7.7	4.3	4.2
IND	1.7	1.7	1.5	2.1	1.7	1.4	2.5	1.2	1.3	1.0
ED	1.4	2.1	1.8	1.7	1.4	2.1	2.1	1.6	1.2	1.4
TD	0.9	0.8	0.9	0.7	0.8	0.9	1.2	1.1	0.6	0.8
SNL	3.2	3.9	3.5	3.7	3.6	3.5	3.7	3.7	2.5	2.4
SFIL	15.1	17.1	18.3	19.3	17.3	16.4	17.9	17.5	12.3	11.2
FLL	11.3	11.4	10.5	12.2	11.3	11.1	12.1	11.0	8.2	7.4
HLL	15.7	14.6	16.7	17.3	16.4	13.9	18.8	15.7	10.5	9.4
TBL	3.4	4.0	3.1	4.6	3.9	3.4	4.3	4.8	2.7	1.9
T4L	5.2	5.3	5.3	6.1	4.7	4.9	6.3	5.6	4.1	3.5
EED	3.6	3.8	4.1	4.7	3.7	3.5	4.4	3.8	2.9	2.9
END	2.3	2.4	2.3	2.9	2.4	2.2	2.6	2.6	1.5	1.6
RW	1.6	1.6	1.6	1.5	1.0	1.8	1.4	2.1	1.1	0.9
RD	1.0	1.1	1.0	2.0	1.1	1.0	2.1	1.2	0.9	0.8
HL2/SVL	0.18	0.17	0.19	0.20	0.19	0.19	0.18	0.18	0.23	0.21
HW/SVL	0.16	0.12	0.15	0.13	0.15	0.14	0.15	0.15	0.17	0.16
HH/HL2	0.51	0.52	0.56	0.49	0.62	0.64	0.67	0.59	0.49	0.55
SNL/HW	0.47	0.62	0.53	0.61	0.54	0.57	0.52	0.54	0.52	0.52
ED/SNL	0.42	0.53	0.53	0.47	0.40	0.59	0.56	0.43	0.47	0.57
ED/HL2	0.18	0.25	0.22	0.19	0.17	0.25	0.24	0.19	0.18	0.23
SVL/MBW	5.90	6.09	5.53	7.08	6.24	6.05	6.47	6.02	6.77	6.81
EED/END	1.57	1.59	1.78	1.62	1.55	1.65	1.74	1.45	1.92	1.83
SVL/HW	6.18	8.14	6.80	7.48	6.86	7.06	6.70	6.83	6.05	6.09
SVL/HL2	5.41	6.04	5.24	4.94	5.35	5.23	5.53	5.44	4.34	4.73
SVL/FLL	3.67	4.45	4.23	3.67	4.01	3.90	3.91	4.21	3.54	3.82
SVL/HLL	2.65	3.48	2.67	2.59	2.78	3.12	2.51	2.99	2.79	3.01

and behind, the tympanum is deeply sunk, not covered with scales, and there is one projecting ear lobule on the anterior edge of the ear opening.

Six infralabials, the sixth being the largest. Mental scale wider than longer with concave posterior margin. Anterior postmental single, large, nearly three times the length of mental, laterally postmental widely in contact with first and second infralabials on both sides, a pair of first chin shields medially contacting each other, laterally in contact with second and third infralabials. The second pair of adjoining chin shields touches the third and fourth infralabials, separated by a subequal cycloid scale. The third pair of adjoining chin shields touches fourth and fifth infralabials, separated by three subequal cycloid scales.

Table 2. Meristic data for the type series *Ablepharus flammeus* sp. n. Abbreviations are listed in the Materials and methods. Data recorded through "/" indicate the value on the right/left side of the head or body.

	ZSI-R_29457	MZMU3656	MZMU3657	MZMU3652	MZMU3658	MZMU3659	MZMU3653	MZMU3660	MZMU3654	MZMU3655
	Holotype ♂	Paratype ♀	Paratype ♂	Paratype ♂	Paratype ♂	Paratype ♂	Paratype ♂	Paratype ♂	Paratype Juv	Paratype Juv
PF	no, wide	no	no, wide	no	touch at one point	no, wide	no	no	no, wide	no, wide
F-SO	1st, 2nd/ 1st, 2nd	1st, 2nd/ 1st, 2nd	1st, 2nd/ 1st, 2nd	1st, 2nd/ 1st, 2nd	1st, 2nd/ 1st, 2nd	1st, 2nd, 3rd/ 1st, 2nd	1st, 2nd/ 1st, 2nd	1st, 2nd/ 1st, 2nd	1st, 2nd/ 1st, 2nd	1st, 2nd/ 1st, 2nd
Nu	4/4	4/4	4/4	4/4	4/4	4/4	4/4	4/4	4/4	4/4
PR	3	3	3	2	3	3	2	3	3	3
PRS	1	1	1	1	1	1	1	1	1	1
SC	5	5	5	5	5	5	5	5	5	5
PO	2	2	2	2	2	2	2	2	2	2
PSO	3	3	3	3	3	3	3	3	3	3
SL	7/7	7/7	7/7	7/7	7/7	7/7	7/7	7/7	7/7	7/7
IF	6/6	6/6	6/6	6/6	6/7	6/6	6/6	6/6	6/6	6/6
PEL	1	2	2	1	1	1	1	1	3	1
MBSR	28	26	28	28	28	28	26	26	26	26
PVSR	54	56	54	54	56	52	54	54	54	54
DBR	4	4	4	4	4	4	4	4	4	4
VSR	62	62	64	60	64	60	60	62	66	66
PrC	2	2	2	2	2	2	2	2	2	2
FL4	12	12	12	12	12	12	12	12	12	12
TL4	16	16	16	16	16	16	16	16	16	16
F-H	no	no	no	no	no	no	no	no	yes	yes
F-E	no	no	no	no	no	no	no	no	no	no

Dorsal scalation heterogeneous, composed of smaller cycloid, imbricate scales laterally and a series of slightly enlarged, broad vertebral scales; the latter include four pairs of nuchals starting from behind parietals and followed by four rows of scales between dark dorsolateral stripes on the upper lateral edges of the body, each nearly half the size of a nuchal scale ending at the level slightly beyond the groin; roughly two to four times larger than the adjoining dorsolateral scales. The paravertebral scale series composed of 54 scales, including nuchals. Scales around the midbody in 28 rows. Dorsal scales smooth, with four barely noticeable obtuse keels, glossy. Scales on lateral aspects of neck and limbs much smaller and more or less similar in shape to those on body flanks. Ventral scales similar in size and shape to those on the flanks; the mid ventral scale series composed of 62 scales when counted from first pair of chin shields (including gulars) to cloaca. Medial pair of precloacal scales enlarged. Tail unregenerate. Tail scales cycloid, smooth, imbricate; all equal in shape except subcaudals, which are greatly widened and by far the largest (twice the size of vertebral row).

The hemipenis has no visible macrostructures or ornaments (Fig. 5). The hemipenis is deeply bilobed, with two equally long, slender, elongated, and symmetrical branches. Length-to-width branch ratio is approx. 3:1. The sulcus spermaticus bifurcation point is close to that of the branching. Thin, well-developed labia surround the sulcus. The sulci open on the tip of the branches of the hemipenis. The labium at the end of the sulci has no terminal awl. The length of the branches (apex) is equal – 2.4 mm; branches

are slightly shorter than the body (truncus + pedicle) of the hemipenis – 3.5 mm. The truncus of the hemipenis bears two approx. 1.5 mm long, clearly visible, flattened, asymmetrical lobes (bulbous lobes, or "fold-lock" according to Eremchenko & Panfilov (1990)). Just above the truncus, on the inner side of the sulcus, each of the branches bears one expanded, flattened leaf-shape, 0.5 mm long lobules, bearing a spike and directed outwards from the branches, in opposite directions relative to each other, The total length of the hemipenes is 5.5 mm.

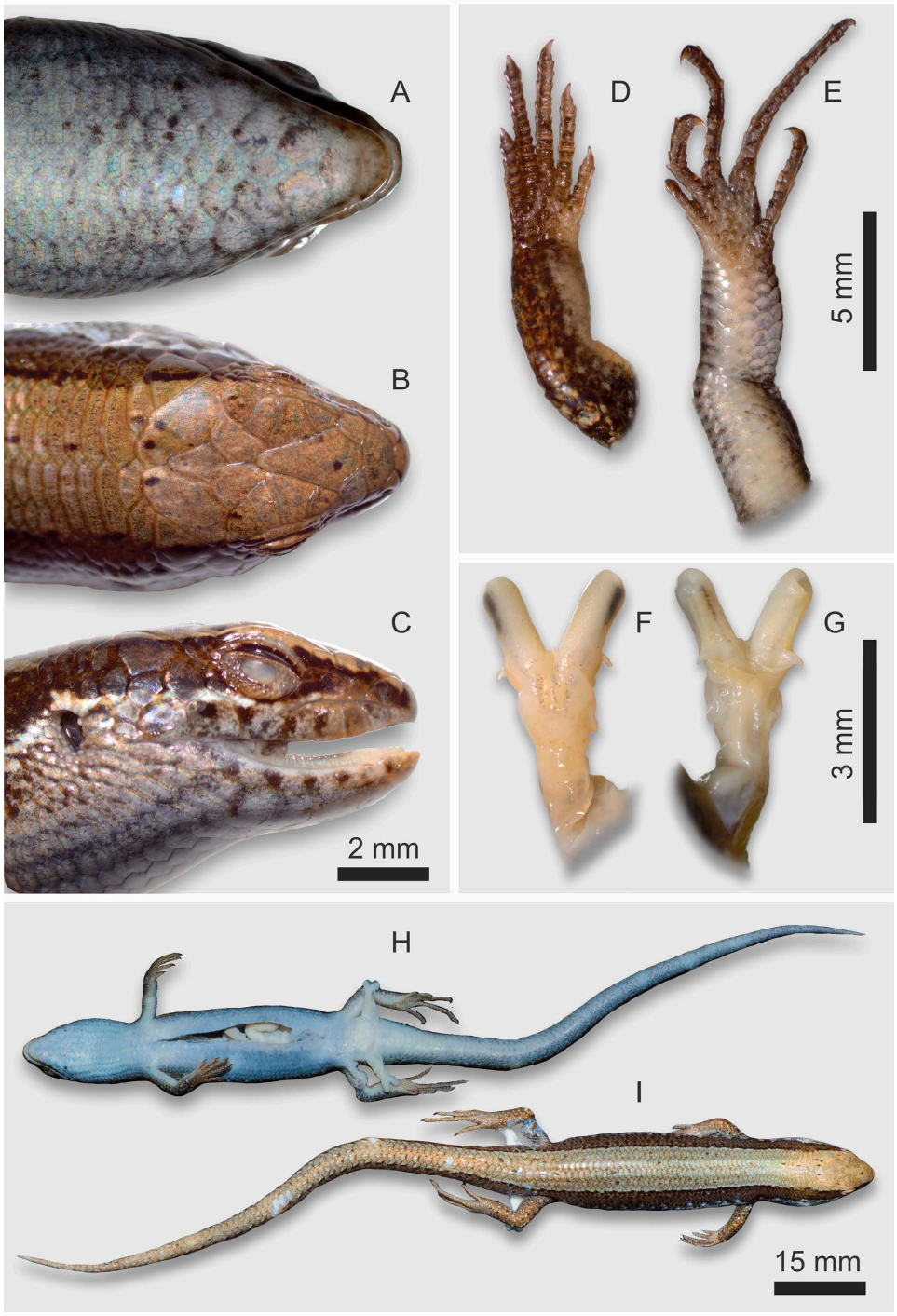

Figure 5. Preserved holotype of *Ablepharus flammeus* sp. n. (ZSI-R-29457, adult) from the type locality of Chopta, Uttarakhand, India: (A) ventral view of head; (B) dorsal view of head; (C) right lateral view of head; (D) ventral view of left forelimb; (E) ventral view of left hindlimb; (F) dorsal view of right hemipenis, fully everted; (G) ventral view of right hemipenis, fully everted; (H) dorsal view of body; (I) ventral view of body. Scale bars: A–C = 2 mm; D, E = 5 mm; F, G = 3 mm; H, I = 10 mm. Photographs by Andrey M. Bragin.

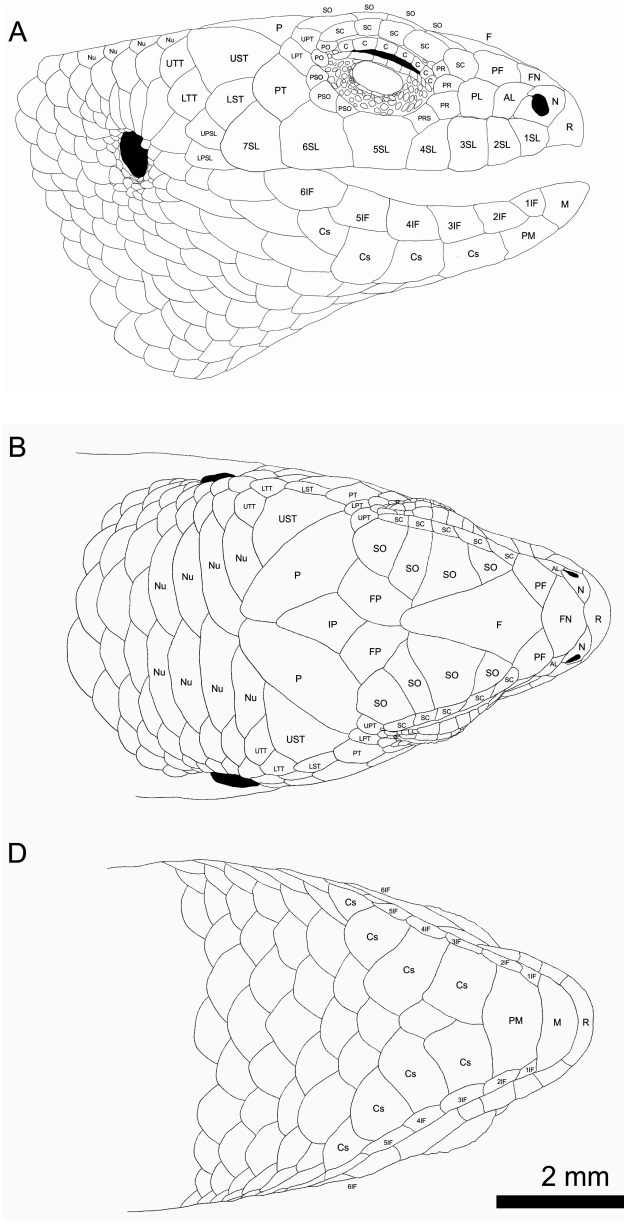

Figure 6. Head scale nomenclature and their positional relationship and size illustrated in a schematic line drawing of the adult male holotype of *Ablepharus flammeus* sp. n. (ZSI-R-29457) (SVL = 41.57 mm) from the type locality of Chopta, Uttarakhand, India: (A) left lateral view; (B) dorsal view; (C) ventral view. Terminology is modified from Ouboter (1986) and Grismer et al. (2019). AL – Anterior loreal; C – ciliary; Cs – chin shield; F – frontal; FN – frontonasal; FP – frontoparietal; IF – infralabial; IP – interparietal; LST – lower secondary temporal; LTT – lower tertiary temporal; LPT – lower pretemporal; LPSL – lower postsupralabial; M – mental; N – nasal; Nu – nuchal; P – parietal; PF – prefrontal; PL – posterior loreal; PM – postmental; PR – preocular; PRS – presubocular; PT – primary temporal; PSO – postsubocular; PO – postocular; R – rostral; SC – supraciliary scales; SL – supralabial; SO – supraocular; UPT – upper pretemporal; UPSL – lower postsupralabial; UST – upper secondary temporal; and UTT – upper tertiary temporal. Drawing by Andrey M. Bragin.

In life (Fig. 7), dorsal surface of the head from green-brown to pale brown, with irregular dark spots; dorsum same as dorsal surface of the head, with rarely dotted two dark vertebral stripes (Figs 3, 7); an additional two thinner broken lines sometimes occurred beside the mid-dorsal line; the dorsal surface of tail pale brown with irregular light and dark spots in two broken lines. Iris dark brown; supralabial and infralabial light greyish white, with regularly distributed dark spots; dorsolateral dark stripe persists from naris along anterior loreal, posterior loreal, and preocular through the eye and lateral side of the trunk until the tip of the tail, with a light narrow border line at the upper edges of the band; lateral dark grey-brown band persists from naris along anterior loreal, posterior loreal, and preocular through the eye and lateral side of the trunk gradually eroding towards the tip of the tail, with a dark narrow border line at the lower edge of the band; a white broken lateral stripe under the dark lateral band from the middle of the lower edge of the eye, gradually eroding towards the tip of tail, with series of dark patches lined under the white stripe. Ventral surfaces of mental, chin and gulars from greyish white to pale blue, gradually turning from dark orange to brick red in males and juveniles, and turning to ochre yellow in females from throat to ventral side of trunk, limbs, and anterior ⅓ tail; posterior ⅔ tail from greyish white to pale blue. Dorsal surface of hands and feet brown with dark spots; ventral surface of hands and feet from pale brown to greyish white.

In preservative (Fig. 5), dorsal surfaces turned from green-brown to pale green; dark spots remain but slightly fade; lateral dark band fades to walnut brown, and the black narrow border lines remain distinct, the dorsolateral stripe acquiring a light border along the upper edge; lateral white stripe under the dark band persisted; all the black spots on head, trunk, tail, and limbs remained; ventral region of the trunk, limbs and ventral of tail faded from dark orange – brick red – ochre yellow to purple blue – light blue.

Variation and sexual dimorphism: The broken dark dorsal line is obscured in some individuals and is represented by dispersed dots. A regenerate tail does not have the character of ventral grayish white to pale blue or orange-red coloration and lateral dark band and becomes a solid beige-brown. There is variability in the following characteristics of head pholidosis: in specimen MZMU3659 frontal is in contact with the first, second and third supraoculars (vs. in contact with the first and second supraoculars in the remaining specimens); in specimen MZMU3658 prefrontals contact each other at one point (vs. the widely separated by frontal in the other specimens); specimens MZMU3652 and MZMU3653 have two preoculars (vs. three preoculars in other specimens); specimen MZMU3658 has seven infralabials on the left side of the head (vs. six infralabials on the both side of head and in other specimens); 70% of specimens have one projecting ear lobule, 20% of specimens – two, and 10% of specimens – three.

Males have more contrasting and bright coloration patterns (Fig. 7). Vivid coloration difference on the ventral surface of body: ventral region of the neck, tail, and limbs of males and juveniles from orange to red, and yellow in females. Based on current data, males have a trend of longer limbs, larger heads, and shorter bodies (lower SVL/FLL, SVL/HLL, SVL/HL2, SVL/HW ratio) than females. Females are larger in SVL (Tables 1, 2).

Comparisons: The new species differs from the species of *Ablepharus* living to the west of the Himalayan region (*Ablepharus alaicus*, *A. anatolicus*, *A. bivittatus* Menetries, 1832, *A. budaki*, *A. chernovi*, *A. darvazi* Eremchenko & Panfilov, 1990, *A. deserti*, *A. eremchenkoi*, *A. grayanus* Stoliczka, 1872, *A. kitaibelii*, *A. lindbergi* Wettstein, 1960, *A. pannonicus*, *A. rueppellii*) in its larger size, longer limbs about the length of the body and, most

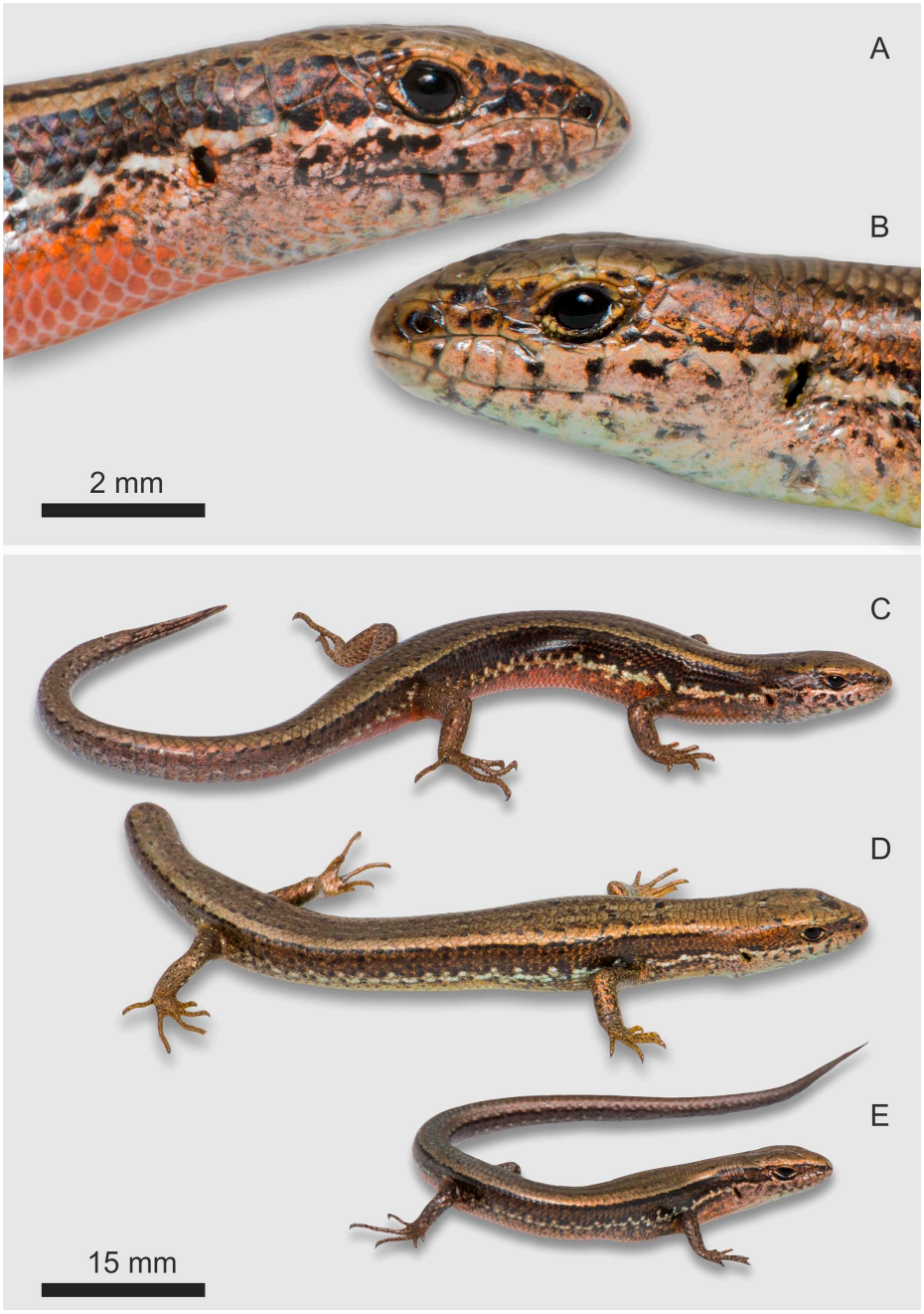

Figure 7. The appearance of type specimens of *Ablepharus flammeus* sp. n. from the type locality of Chopta, Uttarakhand, India in life: (A) lateral view of the head of male (paratype, MZMU3660); (B) lateral view of the head of female (paratype, MZMU3656); (C) dorsolateral view of male (paratype, MZMU3660); (D) dorsolateral view of female (paratype, MZMU3656); (E) dorsolateral view of juvenile (paratype, MZMU3654). Scale bars: A, B = 2 mm; C–E = 15 mm. Photographs by Andrey M. Bragin.

importantly, the presence of a movable lower eyelid with relatively small transport window (vs. fused (*Ablepharus anatolicus*, *A. bivittatus*, *A. budaki*, *A. chernovi*, *A. darvazi*, *A. deserti*, *A. grayanus*, *A. kitaibelii*, *A. lindbergi*, *A. pannonicus*, *A. rueppellii*) or partially fused (*Ablepharus alaicus*, *A. eremchenkoi*) lower eyelid completely covered by transparent window).

Morphological characters that distinguish *A. flammeus* from other ablepharine skinks of the Himalayas region are summarized in Tables 3–5. An important difference between the new species is its geographic range. *Ablepharus flammeus* is diagnosed from *A. mahabharatus, A. nepalensis, A. ladacensis*, and *A. capitaneus* by having fewer than 30 midbody scale rows (28 vs. 30–34), four rows of scales between dark dorsolateral stripes (vs. six rows), longitudinally oriented large femoral scales (vs. a group of femoral scales oriented across the thigh with small upper femoral scalation), presence or lower number of projecting ear lobules (vs. absence in *A. nepalensis* and *A. mahabharatus* and approx. 3 projecting ear lobules in *A. ladacensis*), and absence of vertebral stripes (vs. presence in *A. ladacensis* and *A. nepalensis*). *Ablepharus flammeus* is diagnosed from *A. sikimmensis* by presence of projecting ear lobules (vs. absence), an average large number of midbody scale rows (27.3 vs. 24.57), large number of ventral scale rows (62.3 vs. 41.08), large number of fourth toe and finger subdigital lamellae (16 vs. 15.17 and 12 vs. 10.7 respectively), and also by the fact that the venter of females does not turn orange or red, like that of males, but remains yellow (vs. orange venter in both males and females). The sibling species of *A. flammeus* is *A. himalayanus* for which cases of sympatry can be found. *Ablepharus flammeus* is diagnosed from *A. himalayanus* by having a smaller number of paravertebral scale rows (54.3 vs. 57.8), ventral scale rows (62.3 vs. 65.2) and projecting ear lobules (1.3 vs. 2.7), smaller body size (SVL) (45.5 mm vs. 68.2 mm), narrower range of midbody scale rows (26–28 vs. 24–32), fourth toe (16 vs. 14–22) and finger (12 vs. 9–13) subdigital lamellae, and fewer cases of contact of frontal with the first, second and third supraoculars (10% vs. 64%). *Ablepharus flammeus* is diagnosed from *A. tragbulensis* by having a smaller number of midbody scale rows (27.3 vs. 31), ventral scale rows (62.3 vs. 71.5), fourth toe subdigital lamellae (16 vs. 21), postmentals (1 vs. 2), infralabials (6 vs. 7), supralabials (7 vs. 8), preoculars (3 vs. 2), smaller head in relation to body length (SVL/HW; SVL/HL2) (7 vs. 9.55; 5.4 vs. 6.81), and absence of dorsal stripes (vs. presence of 10–11 stripes).

Distribution: The species is known only from two places in Chopta region in Uttarakhand state in northern India: from Duggal Bittha village (30.48° N, 79.17° E) at an elevation of 2,520 m a.s.l. and from Green Valley near of Tungnath Temple (30.48° N, 79.20° E) at an elevation of 3,305 m a.s.l. in the type locality (Figs 1, 4).

Natural history notes and conservation status: At the type locality, *A. flammeus* inhabits a wide range of micro relief and plant communities (Fig. 4), ranging from gentle slopes covered with multilayer high-stem polydominant deciduous forests formed by *Quercus semecarpifolia, Q. floribunda, Acer acuminatum, Aesculus indica, Q. leucotrichophora* and *Alnus nepalensis* at an altitude of 2,520 m a.s.l. through steep slopes covered with patches of low mixed forest formed by *Abies pindrow*, *Quercus semecarpifolia, Q. floribunda, Rhododendron arboreum,* etc. to subalpine and alpine meadows at an altitude of 3,305 m a.s.l. During the study period, daytime temperatures were in the range of 12–15 °C, and night temperatures dropped below -3 °C. However, in the morning hours (8:00 am) the lizards were active and stayed on the forest edges free of vegetation in the leaf litter, forming fairly dense clusters of different ages and genders of individuals. In subalpine meadows, individual specimens were found active near large *Rhododendron arboreum* bushes on the border of snowfields. No other species of reptiles or amphibians were found in the same area during the study period. The ecology of this species remains largely unknown.

The habitat of the skinks is stable since the lizard's current distribution largely overlaps with areas used for ecotourism and pilgrimage; there is practically no agricultural activity in the type locality, and lizards are also found in disturbed plant communities and anthropogenic landscapes; and there is no hunting or collection pressure on this species. However, given such little data on the distribution of the species, it may be a local endemic like *A. nepalensis*, *A. mahabharatus,* or *A. tragbulensis*, or on the contrary, it can have a much wider distribution in the hills of Eastern and Western Himalaya as suggested by the previous works (Mirza et al. 2022, Bragin et al. 2024). The new species *A. flammeus* should also be considered Data Deficient (DD) according to the criteria of the IUCN (2025). Further comprehensive research is required to establish the actual limits of distribution and other data necessary to meaningfully assess threat status (Myers et al. 2001).

Discussion

In the present study, we report on a previously unknown lineage of Himalayan ablepharine skinks of the genus *Ablepharus*. According to our mtDNA-based genealogy, the newly discovered species *Ablepharus flammeus* forms a highly divergent lineage of ablepharine skinks, which are suggested as the sister lineages to all other members of the *A. tragbulensis* – *A. ladacensis* species complex (see Fig. 2). The new species may also be distinguished from congeners by a significant divergence in 16S rRNA and cyt b gene sequences (with p = 5.5–11.6% in 16S rRNA and p = 14.6–22.0% in cyt b), which are higher than the genetic distances between many other recognized species of the genus *Ablepharus* (see Supplementary Table S4). The mtDNA-based genealogy is in congruence with results from our earlier analysis by Bragin et al. 2024, which recovered the same clades within Himalayan ablepharine skinks. Based on our observations, *Ablepharus flammeus* is known only from the Chopta region in Uttarakhand, India. Our work raises the

Table 3. Comparative characters between *Ablepharus flammeus* sp. n., *A. tragbulensis, A. himalayanus, A. ladacensis, A. capitaneus, A. sikimmensis, A. nepalensis, A. mahabharatus.* Abbreviations are listed in the Materials and methods. The data is presented in the following form: minimum value–maximum value (average ± standard deviation). n – sample size, n.a. – data not available. Morphological measurements given in millimeters. Elev. – Elevation in m a.s.l.; Rep. – Reproduction.

	A. flammeus sp. n.	*A. tragbulensis*	*A. himalayanus*	*A. ladacensis*	*A. capitaneus*	*A. sikimmensis*	*A. nepalensis*	*A. mahabharatus*
Reference	This study	Das et al. 1998	Ouboter 1989, Eremchenko in Schleich & Kästle 2002	Ouboter 1989, Eremchenko in Schleich & Kästle 2002	Ouboter 1989, Eremchenko in Schleich & Kästle 2002	Ouboter 1989, Eremchenko in Schleich & Kästle 2002	Eremchenko et al. 1998	Eremchenko et al. 1998
	n=10	n=5	n=71	n=101	n=9	n=141	n=5	n=2
Elev.	2520–3305	2740	2600–3100	2590–5490	1100–2100	1200–3200	1500–1580	1950–2300
Rep.	none	none	viviparous–oviparous	viviparous	oviparous	oviparous	none	none
SVL	41.6–50.6 (45.5±7.4)	44.2–56.5 (49.72±2.07)	66.8–78.5 (68.2±10)	36–70.5 (45.8±9.5)	*–53.7 (43.8±9.3)	*–55.8 (39.1±8.7)	32.5–41 (35.3±3.58)	30–44 (37±9.9)
TaL	52.6–68.3 (59.2±10.0)	69.5	n.a.	n.a.	n.a.	n.a.	58–69 (63.5±7.78)	– (48±0)
TaW	3.7–5.3 (4.4±0.8)	4.5–4.9 (4.7±0.28)	n.a.	n.a.	n.a.	n.a.	n.a.	n.a.
AGD	24.4–31.3 (27.6±4.8)	n.a.	n.a.	n.a.	n.a.	n.a.	14–20 (17.14±2.78)	13–22 (17.5±6.36)
HL1	5.1–8.2 (7.1±1.3)	6.2–8.7 (7.45±1.77)	n.a.	n.a.	n.a.	n.a.	n.a.	n.a.
HL2	7.7–9.1 (8.4±0.9)	n.a.	n.a.	n.a.	n.a.	n.a.	7.7–8.7 (7.98±0.41)	7.2–9.5 (8.35±1.63)
IOD	3.2–4.3 (3.6±0.6)	3.8–4 (3.9±0.14)	n.a.	n.a.	n.a.	n.a.	n.a.	n.a.
SEL	8.5–9.4 (9.0±1.1)	n.a.	n.a.	n.a.	n.a.	n.a.	n.a.	n.a.
HW	6.0–7.1 (6.5±0.8)	4.9–5.6 (5.25±0.49)	n.a.	n.a.	n.a.	n.a.	5.5–6.2 (5.9±0.25)	5–6 (5.5±0.71)
HH	3.9–5.7 (4.8±0.8)	4.1–4.5 (4.3±0.28)	n.a.	n.a.	n.a.	n.a.	n.a.	n.a.
MBW	6.3–8.3 (7.4±1.4)	5.7–7.5 (6.6±1.27)	n.a.	n.a.	n.a.	n.a.	n.a.	n.a.
IND	1.2–2.5 (1.7±0.5)	1.8–2 (1.9±0.14)	n.a.	n.a.	n.a.	n.a.	n.a.	n.a.
ED	1.4–2.1 (1.8±0.3)	2.2–2.5 (2.35±0.21)	n.a.	n.a.	n.a.	n.a.	n.a.	n.a.
TD	0.7–1.2 (0.9±0.2)	0.8–0.8 (0.8±0)	n.a.	n.a.	n.a.	n.a.	n.a.	n.a.
SNL	3.2–3.9 (3.6±0.5)	3.9–4.2 (4.05±0.21)	n.a.	n.a.	n.a.	n.a.	n.a.	n.a.
SFIL	15.1–19.3 (17.3±2.6)	n.a.	n.a.	n.a.	n.a.	n.a.	n.a.	n.a.
FLL	10.5–12.2 (11.4±1.6)	12–13.3 (12.65±0.92)	n.a.	n.a.	n.a.	n.a.	9–11 (9.64±0.86)	9.8–11 (10.4±0.85)
HLL	13.9–18.8 (16.1±2.9)	17.8–18.7 (18.25±0.64)	n.a.	n.a.	n.a.	n.a.	13–17 (14.38±1.52)	13.8–17.5 (15.65±2.62)
TBL	3.1–4.8 (3.9±0.9)	5.8–6.3 (6.05±0.35)	n.a.	n.a.	n.a.	n.a.	n.a.	n.a.
T4L	4.7–6.3 (5.4±0.9)	n.a.	n.a.	n.a.	n.a.	n.a.	n.a.	n.a.
EED	3.6–4.7 (4.0±0.6)	3.2–3.7 (3.45±0.35)	n.a.	n.a.	n.a.	n.a.	n.a.	n.a.
END	2.2–2.9 (2.5±0.4)	2.6–2.7 (2.65±0.07)	n.a.	n.a.	n.a.	n.a.	n.a.	n.a.
RW	1.4–2.1 (1.7±0.3)	1.7–1.7 (1.7±0)	n.a.	n.a.	n.a.	n.a.	n.a.	n.a.
RD	1.0–2.1 (1.3±0.5)	0.9–1 (0.95±0.07)	n.a.	n.a.	n.a.	n.a.	n.a.	n.a.

Table 3 continued

Reference	*A. flammeus* sp. n.	*A. tragbulensis*	*A. himalayanus*	*A. ladacensis*	*A. capitaneus*	*A. sikimmensis*	*A. nepalensis*	*A. mahabharatus*
	This study	Das et al. 1998	Ouboter 1989, Eremchenko in Schleich & Kästle 2002	Ouboter 1989, Eremchenko in Schleich & Kästle 2002	Ouboter 1989, Eremchenko in Schleich & Kästle 2002	Ouboter 1989, Eremchenko in Schleich & Kästle 2002	Eremchenko et al. 1998	Eremchenko et al. 1998
	n=10	n=5	n=71	n=101	n=9	n=141	n=5	n=2
HL2/SVL	0.17–0.23 (0.19±0.02)	0.14–0.15 (0.15±0.01)	n.a.	n.a.	n.a.	n.a.	n.a.	n.a.
HW/SVL	0.12–0.17 (0.14±0.01)	0.1–0.11 (0.1±0.01)	n.a.	n.a.	n.a.	n.a.	n.a.	n.a.
HH/HL2	0.49–0.67 (0.57±0.07)	0.52–0.66 (0.59±0.1)	n.a.	n.a.	n.a.	n.a.	n.a.	n.a.
SNL/HW	0.47–0.62 (0.55±0.04)	0.75–0.8 (0.77±0.03)	n.a.	n.a.	n.a.	n.a.	n.a.	n.a.
ED/SNL	0.4–0.59 (0.49±0.07)	0.56–0.6 (0.58±0.02)	n.a.	n.a.	n.a.	n.a.	n.a.	n.a.
ED/HL2	0.17–0.25 (0.21±0.03)	0.29–0.35 (0.32±0.05)	n.a.	n.a.	n.a.	n.a.	n.a.	n.a.
SVL/ MBW	5.53–7.08 (6.17±0.48)	7.53–7.75 (7.64±0.16)	n.a.	n.a.	n.a.	n.a.	n.a.	n.a.
EED/END	1.45–1.92 (1.62±0.14)	1.23–1.37 (1.3±0.1)	n.a.	n.a.	n.a.	n.a.	n.a.	n.a.
SVL/HW	6.18–8.14 (7±0.65)	9.02–10.09 (9.55±0.76)	*–* (6.9±0.7)	*–* (6.7±0.5)	*–* (8±0.7)	*–* (6.7±0.6)	5.51–6.61 (6.02±0.41)	6–7.33 (6.67±0.94)
SVL/HL2	4.94–6.04 (5.4±0.47)	6.49–7.13 (6.81±0.45)	*–* (5.5±0.6)	*–* (5.1±0.6)	*–* (6.5±0.6)	*–* (5.3±0.7)	4.17–4.71 (4.42±0. 24)	4.17–4.63 (4.4±0.33)
SVL/FLL	3.7–4.5 (4±0.3)	3.68–4.25 (3.97±0.4)	*–* (3.7±0.4)	*–* (3.2±0.3)	*–* (4.1±0.2)	*–* (3.8±0.4)	3.61–3.73 (3.66±0.05)	3.06–4 (3.53±0.66)
SVL/HLL	2.5–3.5 (2.9±0.3)	2.48–3.02 (2.75±0.38)	*–* (2.7±0.3)	*–* (2.5±0.2)	*–* (2.7±0.2)	*–* (2.7±0.3)	2.32–2.63 (2.46±0.11)	2.17–2.51 (2.34±0.24)

total number of species of the genus *Ablepharus* from 20 to 21; *Ablepharus flammeus* represents the seventh *Ablepharus* species known for India. Despite the recent significant progress, our knowledge of molecular phylogeny, classification, and distribution of Himalayan ablepharine skinks remains incomplete. There is an urgent need to clarify the conservation status of newly described populations. The new species *Ablepharus flammeus* may well represent an example of an endemic confined to a specific plant community of high-mountain hard-leaved deciduous forests, where anthropogenic activities can have a destructive impact.

The discovery of new ablepharine skinks in the Himalayan region was not unexpected. In recent years, skinks have been described with unprecedented frequency (Chapple et al. 2023). However, until the present study, starting from the end of the 20th century, the species diversity of the Himalayan representatives of the genus *Ablepharus* had remained unchanged (Eremchenko et al. 1998, Eremchenko in Schleich & Kästle 2002). The ability to at least quadruple the known diversity of ablepharine skinks has been demonstrated by earlier research (Bragin et al. 2024). However, the information presented here is still based on only a few trips to various locations inside this enigmatic mountain region. As research into the Himalayan Mountain subsystems continues, a far greater number of species could be expected.

It is also crucial to conduct further research on the genetics, morphology, and ecology of the newly discovered and existing species. Because of our limited collection of genetic markers and the resulting sequence database for the populations under study, we are unable to fully explain the evolutionary history of ablepharine skinks. Identification of even known *Ablepharus* species by morphological characters is also significantly difficult. To date, there are only two identification keys, both incomplete, including either only representatives of the *Ablepharus* species to the west of the Himalayas (Eremchenko & Szczerbak 1986), or only the *Ablepharus* species living in the territory of Nepal (Eremchenko in Schleich & Kästle 2002). Both identification keys are incomplete and contain a number of highly variable morphological characters. Lastly, a reassessment of the current synonyms of the known species would be imperative.

The available descriptions of ablepharine skink species are also quite fragmented in terms of the choice of methods for calculating meristic morphological characters as well as the choice of sets of these characters. For instance, it is necessary to recheck specimens of *A. tragbulensis* because it is doubtful according to Das et al. (1998) whether this species of ablepharine skink has two postmentals and eight supra- and seven infralabial scales as opposed to all other species' single, unpaired postmental and seven supra- and six infralabials. Other discrepancies are possible. We reiterate the

Table 4. Summary diagnostic characters among *Ablepharus flammeus* sp. n., *A. tragbulensis, A. himalayanus, A. ladacensis, A. capitaneus, A. sikimmensis, A. nepalensis, A. mahabharatus.* Abbreviations are listed in the Materials and methods. The data is presented in the following form: minimum value–maximum value (average ± standard deviation). n – sample size, n.a. – data not available. Data recorded through "/" indicate the value on the right/left side of the head or body. Elev. – Elevation in m a.s.l.; Rep. – Reproduction.

	A. flammeus sp. n.	*A. tragbulensis*	*A. himalayanus*	*A. ladacensis*	*A. capitaneus*	*A. sikimmensis*	*A. nepalensis*	*A. mahabharatus*
Reference	This study	Das et al. 1998	Ouboter 1989, Eremchenko in Schleich & Kästle 2002	Ouboter 1989, Eremchenko in Schleich & Kästle 2002	Ouboter 1989, Eremchenko in Schleich & Kästle 2002	Ouboter 1989, Eremchenko in Schleich & Kästle 2002	Eremchenko et al. 1998	Eremchenko et al. 1998
	n=10	n=5	n=71	n=101	n=9	n=141	n=5	n=2
Elev.	2520–3305	2740	2600–3100	2590–5490	1100–2100	1200–3200	1500–1580	1950–2300
Rep.	None	none	viviparous–oviparous	viviparous	oviparous	oviparous	none	none
PF	no, or rarely touch in one point	n.a.	n.a.	no, or rarely touch in one point or wide contact	n.a.	n.a.	no	no
F-SO	10%–1st, 2nd, 3rd/ 1st, 2nd, 3rd; 90%–1st, 2nd/ 1st, 2nd	n.a.	64%–1st, 2nd, 3rd/ 1st, 2nd, 3rd; 36%–1st, 2nd/ 1st, 2nd	97%–1st, 2nd, 3rd/ 1st, 2nd, 3rd; 3%–1st, 2nd/ 1st, 2nd	1st, 2nd/ 1st, 2nd	1st, 2nd/ 1st, 2nd	1st, 2nd/ 1st, 2nd	50%–1st, 2nd, 3rd/ 1st, 2nd, 3rd; 50%–1st, 2nd/ 1st, 2nd
Nu	4/4 (4±0)	n.a.	n.a.	3–4/3–4 (3.7±0.9)	3–4/3–4 (3.3±0.6)	3–4/3–4 (3.1±0.9)	3–4/3 (–)	3–4/4–4.5 (–)
PR	2–3 (2.8±0.4)	2 (2±0)	n.a.	n.a.	n.a.	n.a.	n.a.	n.a.
SC	5 (5±0)	n.a.	3–7 (5.5±0.8)	5–8 (6.2±0.7)	5–7 (6.1±0.4)	4–8 (5.8±0.6)	n.a.	7 (7±0)
C	not thickened	not thickened	47% distinctly thickened; 32% slightly thickened	distinctly thickened, the last but one ciliar is very narrow	not thickened	not thickened	n.a.	n.a.
PO	2 (2±0)	3 (3±0)	3–5 (4.5±0.6) (PO + PSO)	3–5 (3.8±0.5) (PO + PSO)	5 (–) (PO + PSO)	4–6 (5±0.3) (PO + PSO)	n.a.	n.a.
PSO	3 (3±0)						2 (2±0)	2 (2±0)
SL	7 (7±0)	8 (8±00)	7 (–)	7 (–)	7 (–)	7 (–)	7 (7±0)	7 (7±0)
Timp	tympanum rounded, deeply sunk, with lobules on the anterior border	tympanum large, slit-like, with lobules on the anterior border	tympanum with lobules on the anterior border	tympanum slit-shaped, deeply sunk, usually with some distinct projecting lobules	tympanum slit-shaped, very small, without projecting lobules	tympanum rounded and very small, deeply sunk, without projecting lobules	tympanum is relatively large, not deeply sunk, without projecting lobules	tympanum relatively large, not deeply sunk, without projecting lobules
PEL	1–3 (1.3±0.7)	present	– (2.7±1.1)	– (3±1.1)	– (0.9±1.5)	n.a.	n.a.	n.a.
IF	6 (6±0)	7 (7±0)	6 (–)	6 (–)	6 (–)	6 (–)	n.a.	n.a.
PM	1 (1±0)	2 (2±0)	n.a.	n.a.	n.a.	n.a.	n.a.	n.a.
MBSR	26–28 (27.3±1.1)	28–34 (31±4.24)	24–32 (27.8±1.9)	28–38 (34.1±1.7)	30–32 (–)	21–29 (24.57±1.5)	30–32 (31.4±0.89)	30 (30±0)
PVSR	52–56 (54.3±1.1)	n.a.	51–62 (57.8±2.8)	58–77 (66.3±4)	62–67 (63.8±1.7)	45–66 (53.9±4.2)	n.a.	n.a.
DBR	4	n.a.	4	6	6	4	6	6
VSR	60–66 (62.3±2.1)	70–73 (71.5±2.12)	57–75 (65.2±4.5)	71–90 (80.2±4.5)	61–72 (65.4±3.2)	33–71 (41.08±4.3)	39–44 (42.2±1.92)	40–43 (41.5±2.12)
PrC	2	2	2	2	2	2	2	2
FL4	12 (12±0)	n.a.	9–16 (12.9±1.5)	13–18 (15.4±1.5)	10–12 (12±–)	9–13 (10.7±1)	n.a.	n.a.

Table 4 continued

	A. flammeus sp. n.	*A. tragbulensis*	*A. himalayanus*	*A. ladacensis*	*A. capitaneus*	*A. sikimmensis*	*A. nepalensis*	*A. mahabharatus*
Reference	This study	Das et al. 1998	Ouboter 1989, Eremchenko in Schleich & Kästle 2002	Ouboter 1989, Eremchenko in Schleich & Kästle 2002	Ouboter 1989, Eremchenko in Schleich & Kästle 2002	Ouboter 1989, Eremchenko in Schleich & Kästle 2002	Eremchenko et al. 1998	Eremchenko et al. 1998
	n=10	n=5	n=71	n=101	n=9	n=141	n=5	n=2
TL4	16 (16±0)	21 (21±0)	14–22 (17.2±1.9)	17–24 (20.6±1.6)	15–17 (17 ±–)	12–18 (15.17±1.1)	15.5–17 (16±0.61)	16.5–17.5 (17±0.71)
F-H	no in adults; yes for juveniles	yes	n.a.	n.a.	n.a.	n.a.	n.a.	n.a.
F-E	no in adults; no in juveniles	n.a.	n.a.	n.a.	n.a.	n.a.	n.a.	n.a.
FemS	femoral scales large and oriented longitudinally	n.a.	femoral scales large and oriented longitudinally	femoral scales large and oriented longitudinally; presence of granulular scales on the upper femoral scalation	a group of femoral scales is oriented across the thigh; upper femoral scales large	femoral scales large and oriented longitudinally	a group of femoral scales is oriented across the thigh; upper femoral scalation small	a group of femoral scales is oriented across the thigh; upper femoral scalation small

necessity of indicating an arbitrary large number of measurements rather than just proportions, ratio (Günther 1864) and ranges of values of metric or meristic characters for all specimens (Ouboter 1986, Das et al. 1998) without supplying data for each specimen, as this impedes future work and renders previously acquired data meaningless. In this paper we provide a template for interpreting the head scalation (see Fig. 6), for its further application to other taxa in ablepharine skinks. At this stage, until a thorough morphological examination of specimens representing the recently discovered genetic lineages of ablepharine skinks has been completed, it is difficult to say which morphological characters are best for identification and have minimal variability. Apparently, the most informative morphological characters for identifying known species are: number of midbody scale rows counted as the number of longitudinal scale rows encircling the body at a point midway between the limb insertions; paravertebral scale rows counted as the number of scales in a line from, but not including, the nuchal scales to a point on the dorsum opposite the vent; transverse dorsal scales rows, counted between the lateral dark bars; ventral scale rows counted as a row of scales between the postmental and the precloacal scales; lamellae under the fingers, the number of fourth toe and finger subdigital lamellae, preoculars, presuboculars, postoculars and postsuboculars, as well as the number and the character of the stripes and bands on the dorsal and lateral sides of body, and the nature of the orange or red coloring of lateral and ventral sides of body of males and females.

High variable morphological characters include the degree of contact of prefrontals with each other and with the frontal; the total number of ciliaries and nuchal scales, and number of nuchal scales on each side of the head counted as the number of the scales between opposing upper secondary temporal on each side of the head that contact the parietals. Morphological characters that were considered utilizing various techniques and, presumably, data that are currently widely dispersed and inappropriate for identification: the number of nuchal scales (Ouboter 1986, Eremchenko & Szczerbak 1986, Eremchenko et al. 1998, Eremchenko in Schleich & Kästle 2002), the number of pairs of chin scales (Das et al. 1998), the number of scales on the lateral side of the body counted from acetabular to glenoid cavities (Günther 1864), and the exact number of separate preoculars and separate presuboculars (in the currently available descriptions we should focus on their total number – preoculars + presuboculars) (Ouboter 1986, Eremchenko in Schleich & Kästle 2002). Expansion of the sampling of known species is necessary to understand the ranges of morphological variability. Furthermore, there are currently no adult specimens available for *A. mahabharatus*. Numerous morphological characters that were thought to be unchangeable later proved to be quite variable, which led researchers to look for more variations in hemipenial, craniological, or osteological structures. For instance, only nine species of ablepharine skinks have comprehensive descriptions of their hemipenes (Eremchenko & Panfilov 1990, Vergilov et al. 2017, Vergilov & Zlatkov 2024). Even though individual Himalayan ablepharine skink representatives appear to be widely distributed, there is a lack of information regarding their ecology, which can potentially be species-specific and can be a major factor in the conservation of known biodiversity. Information on reproduction strategies is thus lacking for the great majority of *Ablepharus* and *Protoblepharus* species found in the Himalayan region. Of particular inter-

Table 5. Summary diagnostic coloration patterns among *Ablepharus flammeus* sp. n., *A. tragbulensis, A. himalayanus, A. ladacensis, A. capitaneus, A. sikimmensis, A. nepalensis, A. mahabharatus*. n – sample size, n.a. – data not available.

	A. flammeus sp. n.	*A. tragbulensis*	*A. himalayanus*	*A. ladacensis*	*A. capitaneus*	*A. sikimmensis*	*A. nepalensis*	*A. mahabharatus*
Reference	This study	Das et al. 1998	Ouboter 1989, Eremchenko in Schleich & Kästle 2002	Ouboter 1989, Eremchenko in Schleich & Kästle 2002	Ouboter 1989, Eremchenko in Schleich & Kästle 2002	Ouboter 1989, Eremchenko in Schleich & Kästle 2002	Eremchenko et al. 1998	Eremchenko et al. 1998
	n=10	n=5	n=71	n=101	n=9	n=141	n=5	n=2
Elev. in m a.s.l.	2520–3305	2740	2600–3100	2590–5490	1100–2100	1200–3200	1500–1580	1950–2300
Dark continuous vertebral stripes	absent or rarely dotted two dark dorsal stripes	ten or eleven sharply defined, alternate dark-brown and grayish-white stripes	absent; rarely dotted stripe or band (specimens from the western region of Nepal)	four diffuse dotted stripes	absent	rarely dotted dark vertebral stripe	narrow dark brown vertebral line	absent
Continuous dorsolateral stripes	black	n.a.	yellow-golden to greyish, rarely diffuse	whitish	whitish, wide, distinct	rarely, golden	absent	diffuse greyish
Dark continuous lateral band	broad dark brown	broad dark brown	distinct dark	dark brown	bronze-brown	distinct brown	blackish brown	wide uniform black
White continuous lateral stripes, bordered the lower edge of dark lateral stripe	clear narrow broken white with an irregular edge	n.a.	present	narrow whitish	present	present; in both sexes becomes orange to red in mating season between arms and legs	narrow white with an irregular edge	straight narrow white
Coloration of the dorsum	light gray-yellow-brown to pale brown	n.a.	bronze-brown	brown to olive	light brown to grayish brown	bronze-brown	light brown	light brown
Coloration of venter	grayish to yellowish white	n.a.	greyish blue	greenish to blue	grayish to yellowish white	white to greenish white, yellow or greyish	grayish greenish	n.a.
coloration of males (or/and females*) during the mating season	venter, lower flanks, neck and ventral region of the tail orange to red	n.a.	lower flanks and ventral region of the tail orange to red, sometimes venter also become orange to red	n.a.	orange venter	orange venter (in both males and females) *; white lateral stripes in both sexes becomes orange to red in mating season between arms and legs*	n.a.	n.a.
Spots on the dorsal side	irregular dark or black spots	n.a.	black spots, sometimes associated with white	n.a.	small, irregularly located black spots	irregular dark or black spots	diffuse light and dark strokes	diffuse small brown specks
Spots along lateral sides	small white dots on the lower edge of the lateral band, sometimes irregularly dotted with black	cream spots	light spots	n.a.	small, brown	small white dots on the lower edge of the lateral band, sometimes irregularly dotted with black	rare light specks	absent
Dark, transverse, subcaudal bars or subcaudal banding	absent	n.a.	absent	absent	absent	absent	absent	absent
Coloration of the crown of the head	several large dark spots	dark brown mottling on a gray forehead	n.a.	with black, brown and whitish specks	n.a.	n.a.	n.a.	n.a.
White stripe under the eye	present	n.a.	present	present	absent	dotted	present	present

est is the pattern of distribution of ablepharine skink species and the relative sizes of their habitats.

We observe a picture that species living predominantly at low altitudes in the pine forest belt have fairly extensive distribution ranges in which there is practically no intraspecific variability. Examples of such species are *A. sikimmensis*, which appears to range from Central Nepal east over 450 km to Sikkim in India (Fig. 1). Sub-specific structure within submontane species is weakly expressed (as in the case of *A. sikimmensis*, where species delimitation analyses tend to group reconstructed mtDNA lineages) (Fig. 2, Supplementary Table S4). Conversely, high-mountain species are examples of confusing species complexes with a high degree of genetic and morphological interspecific distances (Fig. 2, Supplementary Table S4). Furthermore, after careful examination, it is quite likely that each of these lineages will have a very small range; currently, this is supported by the species *Ablepharus flammeus*, *A. nepalensis*, and *A. tragbulensis*, which are only known from a few locations and are not found anywhere else. The low-elevation zones are a barrier for high-elevation endemics that are restricted in distribution in the sky islands.

Numerous undescribed lineages of the *A. ladacensis* and *A. himalayanus* species complexes will probably exhibit a comparable distribution (Fig. 1). This distribution is likely since ancestral lineages that colonized the Himalayan foothills either remained in them or moved up, where conditions on individual peaks can significantly vary. In essence, individual peaks acted as "sky islands" well isolated by growing gorges and glaciers, where newly arrived lineages underwent a process of gradual speciation. Thus, on individual peaks in one region, we can find several species of one species complex. In contrast, in the same region, all lower latitudes will be inhabited by another but only one species (Fig. 1). It is necessary to understand that the peak values for genus *Ablepharus* are the maximum among skinks (Chapple et al. 2023), and with such a scatter of altitudes, the boundaries between ancestral lineages could largely serve as the boundaries of plant communities in altitudinal zones. Clade 3 (Fig. 2), which included mid-mountain species like *A. sikimmensis* and *A. mahabharatus*, is likely a better example of such speciation because *A. mahabharatus*, inhabiting altitudes between 1,950 to 2,300 m a.s.l., is found to be more genetically homogeneous, while *A. sikimmensis* that reach altitudes of up to 3,200 m a.s.l. tends to split into several poorly distinguishable mitochondrial lineages, where deeper lineages are found in the highlands, while outer ones inhabit foothill habitats.

It is possible that individual ancestral lineages could have reached some areas of the mountain ranges independently, after the colonization of the lower heights by their relatives. This hypothesis seems more logical than the hypothesis of diversification of taxa as the Himalayas grew, given the dating of colonization by ablepharine skinks of the Sino-Japanese distribution range (Ghosh et al. 2023) and the association of most of the basal lineages of ablepharine skinks and their Lygosominae relatives with humid forests (Ouboter 1986, Eremchenko & Szczerbak 1986, Mirza et al. 2022), most of the flora of which consists of immigrated plant taxa that have evolved and diversified over millions of years following the Himalayan formation (Singh & Singh 1987, Pandit & Kumar 2013, Pandit et al. 2014, Manish & Pandit 2018). The data obtained in this research greatly complicates the hypothesis put forth by Ouboter (1986) and Eremchenko & Szczerbak (1986) regarding the invasion of the Himalayas by three lineages (corresponding to the ancestral lineages of *A. sikimmensis*, *A. himalayanus*, and *A. ladacensis*), and their subsequent expansion into the Eastern, Central, and Western Himalayan regions, respectively. We observed that far more intricate taxonomic diversity that has gone largely unreported, with a complicated web of habitats that include poorly understood sympatric zones and unexplored mechanisms of potential hybridization. More samples from still inadequately explored Himalayan regions (particularly from Ladakh and Sikkim in India, Bhutan, and Eastern and Western Nepal) and more genetic markers are needed to provide a more precise biogeographical scenario.

Acknowledgements

The first author deeply appreciates the friendship and unwavering support of his companions, Platon V. Yushchenko and Yulia D. Kozhevnikova, during the journey to the Himalayan peaks, without whom the new species would not have been discovered and described. AMB is also eternally grateful to Rajiv Bisht Puran Singh and his wonderful family, who provided shelter and all possible assistance and support during his stay in Uttarakhand. We thank Alexey V. Trofimets (member of MSU HerpLab) for his support and assistance. AMB and NAP are grateful to Andrei N. Kuznetsov (JVRTSTRC, Hanoi) for his long-standing support and encouragement. We thank Pratyush P. Mohapatra (ZSI, Kolkata) for his assistance with the registration of the holotype. ZAM acknowledges the Max Planck Society for support. We are grateful to the anonymous reviewers for their helpful comments, which enabled us to improve the previous version of the manuscript. This work was supported by the Russian Science Foundation to NAP (Grant No. 22-14-00037-P, molecular and data analysis).

References

Ankita, R., A. Bharti, V. Kumar & D. Kumar (2017): The preliminary molecular study of four skink species in Rajaji Tiger Reserve (RTR), Uttarakhand, using 12S rRNA mitochondrial locus. – Mitochondrial DNA Part B, **2**: 495–499.

Bragin, A. M., S. L. Litvinchuk, L. J. Borkin, D. A. Melnikov, D. V. Skorinov, D. Jablonski, R. Masroor, H. T. Lalremsanga, Z. A. Mirza, C. Dufresnes & N. A. Poyarkov (2024): Hidden on the roof of the world: mitochondrial data reveals exceptional genetic diversity of Himalayan ablepharine skinks (Reptilia: Scincidae). – Russian Journal of Herpetology, **31**: 351–368.

Chapple, D. G., A. Slavenko, R. Tingley, J. E. Farquhar, M. Camaiti, U. Roll & S. Meiri (2023): Built for success: distribution, morphology, ecology and life history of the world's skinks. – Ecology and Evolution, **13**: e10791.

Che, J. K., F. Yan & Y. Zhang (2020): Amphibians and reptiles in Tibet – diversity and evolution. – Science Press, Beijing.

Das, I., B. Dattagupta & N. Gayen (1998): Systematic status of *Lygosoma himalayanum tragbulensis* Alcock, "1897" 1898 (Sauria:

Scincidae) collected by the Pamir boundary commission, 1885. – Russian Journal of Herpetology, **5**: 147–150.

De Queiroz, K. (2007): Species concepts and species delimitation. – Systematic Biology, **56**: 879–886.

Eremchenko, V. K. (1992): On systematics of *Asymblepharus ladacensis* (Günther, 1864) (Sauria: Scincidae, Lygosominae). – pp. 58–65 in: Eremchenko, V. K., A. M. Panfilov & E. I. Tsarinenko (eds): Research conspectus on cytogenetics and systematics of some Asian species of the Scincidae and Lacertidae. – Ilim Press, Bishkek.

Eremchenko, V. K. (2002): Family Scincidae (Skinks). – pp. 723–768 in: Schleich, H. H. & W. Kästle (eds): Amphibians and Reptiles of Nepal. Biology, Systematics, Field Guide. – ARG Ganther Verlag KG, Ruggell.

Eremchenko, V. K. & A. M. Panfilov (1990): *Ablepharus darvazi* sp. nov. – new species *Ablepharus* (Sauria, Scincidae) from Tadjikistan. – Izvestiya Akademii Nauk Kirgizskoi SSR, Khimiko-tekhnologicheskie biologicheskie nauki, **4**: 56–63.

Eremchenko, V. K. & N. N. Szczerbak (1986): Ablepharine lizards of the USSR and adjacent countries. – Frunze, Ylym Publ.

Eremchenko, V. K., N. Helfenberger, K. B. Shah & A. M. Panfilov (1998): Two new species of skinks (Scincidae: Lygosominae) from Nepal. – Vestnik Natsionalnoi Akademii Nauk Kyrgyzskoi Respubliki, **4**: 41–45.

Ghosh, A., M. Sil, K. B. Ukuwela & A. Datta-Roy (2023): Independent origins or single dispersal? Phylogenetic study supports early Cenozoic origin of three endemic Indo-Sri Lankan Lygosomine skink genera. – Zoologica Scripta.

Grismer, L. L., P. L. Wood, E. S. H. Quah, S. Anuar, N. A. Poyarkov, T. Neang, N. L. Orlov, P. Thammachoti & H. Seiha (2019): Integrative taxonomy of the Asian skinks *Sphenomorphus stellatus* (Boulenger, 1900) and *S. praesignis* (Boulenger, 1900), with the resurrection of *S. annamiticus* (Boettger, 1901) and the description of a new species from Cambodia. – Zootaxa, **4683**: 381–411.

Günther, A. C. L. G. (1864): The Reptiles of British India. – Ray Society, London.

Hall, T. A. (1999): BioEdit: a user-friendly biological sequence alignment editor and analysis program for Windows 95/98/NT. – Nucleic Acids Symposium Series, **41**: 95–98.

Hedges, S. B. (2014): The high-level classification of skinks (Reptilia, Squamata, Scincomorpha). – Zootaxa, **3765**: 317–338.

Huelsenbeck, J. P. & D. M. Hillis (1993): Success of phylogenetic methods in the four-taxon case. – Systematic Biology, **42**: 247–264.

IUCN (2025): The IUCN Red List of Threatened Species. Version 2024-2. – Available online at https://www.iucnredlist.org.

Katoh, K., K. Misawa, K. Kuma & T. Miyata (2002): MAFFT: a novel method for rapid multiple sequence alignment based on fast Fourier transform. – Nucleic Acids Research, **30**: 3059–3066.

Kumar, S., G. Stecher, M. Li, C. Knyaz & K. Tamura (2018): MEGA X: Molecular Evolutionary Genetics Analysis across computing platforms. – Molecular Biology and Evolution, **35**: 1547–1549.

Lanfear, R., B. Calcott, S. Y. W. Ho & S. Guindon (2012): PartitionFinder: combined selection of partitioning schemes and substitution models for phylogenetic analyses. – Molecular Biology and Evolution, **29**: 1695–1701.

Macey, J. R., J. A. Schulte, J. L. Strasburg, J. A. Brisson, A. Larson, N. B. Ananjeva, Y. Wang, J. F. Parham & T. J. Papenfuss (2006): Assembly of the eastern North American herpetofauna: new evidence from lizards and frogs. – Biology Letters, **2**: 388–392.

Manish, K. & M. K. Pandit (2018): Geophysical upheavals and evolutionary diversification of plant species in the Himalaya. – PeerJ, **6**: e5919.

Myers, N., R. A. Mittermeier, C. G. Mittermeier, G. A. B. da Fonseca & J. Kent (2000): Biodiversity hotspots for conservation priorities. – Nature, **403**: 853–858.

Mirza, Z. A., A. M. Bragin, H. Bhosale, G. G. Gowande, H. Patel & N. A. Poyarkov (2022): A new ancient lineage of ablepharine skinks (Sauria: Scincidae) from eastern Himalayas with notes on origin and systematics of the group. – PeerJ, **10**: e12800.

Nguyen, L. T., H. A. Schmidt, A. von Haeseler & B. Q. Minh (2015): IQ-TREE: a fast and effective stochastic algorithm for estimating maximum-likelihood phylogenies. – Molecular Biology and Evolution, **32**: 268–274.

Ouboter, P. E. (1986): A revision of the genus *Scincella* (Reptilia, Sauria, Scincidae) of Asia, with some notes on its evolution. – Zoologische Verhandelingen, **229**: 1–66.

Pandit, M. K. & V. Kumar (2013): Land-use change and conservation challenges in the Indian Himalaya: Past, present, and future. – pp. 121–133 in: Sodhi, N. S., L. Gibson & P. H. Raven (eds): Conservation biology: Voices from the tropics: Wiley-Blackwell.

Pandit, M. K., K. Manish & L. P. Koh (2014): Dancing on the roof of the world: ecological transformation of the Himalayan landscape. – BioScience, **64**: 980–992.

Puillandre, N., S. Brouillet & G. Achaz (2021): ASAP: assemble species by automatic partitioning. – Molecular Ecology Resources, **21**: 609–620.

Ronquist, F. & J. P. Huelsenbeck (2003): MrBayes 3: Bayesian phylogenetic inference under mixed models. – Bioinformatics, **19**: 1572–1574.

Russell, D. W. & J. Sambrook (2001): Molecular Cloning: A Laboratory Manual. – Cold Spring Harbor Laboratory Press, Cold Spring Harbor, NY.

Singh, J. & S. Singh (1987): Forest vegetation of the Himalaya. – The Botanical Review, **53**: 80–192.

Uetz, P., P. Freed & J. Hošek (eds) (2025): The Reptile Database. – Available from: http://www.reptile-database.org, accessed 8 August 2025.

Vergilov, V. S., B. P. Zlatkov & N. D. Tzankov (2017): Hemipenial differentiation in the closely related congeners *Ablepharus kitaibelii* (Bibron & Bory De Saint-Vincent, 1833), and *Ablepharus budaki* (Göçmen, Kumlutaş & Tosunoğlu, 1996) (Squamata: Sauria: Scincidae). – Herpetozoa, **30**: 39–48.

Vergilov, V. S. & B. P. Zlatkov (2024): Morphology of hemipenes and its taxonomic implication in the fused eyelids species of the genus *Ablepharus* (Squamata: Scincidae). – Journal of Comparative Zoology (Zoologischer Anzeiger), **312**: 79–91.

Weng, S. Y., S. Huang, L. Yang, L. F. Peng, C. Wei & J. C. Li (2021): The complete mitochondrial genome of *Asymblepharus himalayanus* (Scincidae; Sauria) and its phylogenetic position within Scincidae. – Mitochondrial DNA Part B, **6**: 3031–3032.

Supplementary data

The following data are available online:

Supplementary Table S1. Localities, voucher information, and GenBank accession numbers for all specimens used in molecular analyses in this study.

Supplementary Table S2. Details of primers used in the study for PCR amplification and sequencing.

Supplementary Table S3. Characteristics of analyzed mtDNA sequences and the proposed optimal evolutionary models for gene and codon partitions as estimated in PartitionFinder v1.0.1.

Supplementary Table S4. Genetic divergence of the genus *Ablepharus* in 16S and cyt b gene sequences.